

**DOT/FAA/TC-20/21**

Federal Aviation Administration  
William J. Hughes Technical Center  
Aviation Research Division  
Atlantic City International Airport  
New Jersey 08405

# **Post-Crash Fire Forensic Analysis on Aerospace Composites – Literature Review**

August 2020

Final report



U.S. Department of Transportation  
**Federal Aviation Administration**

## NOTICE

This document is disseminated under the sponsorship of the U.S. Department of Transportation in the interest of information exchange. The U.S. Government assumes no liability for the contents or use thereof. The U.S. Government does not endorse products or manufacturers. Trade or manufacturers' names appear herein solely because they are considered essential to the objective of this report. The findings and conclusions in this report are those of the author(s) and do not necessarily represent the views of the funding agency. This document does not constitute FAA policy. Consult the FAA sponsoring organization listed on the Technical Documentation page as to its use.

This report is available at the Federal Aviation Administration William J. Hughes Technical Center's Full-Text Technical Reports page: [actlibrary.tc.faa.gov](http://actlibrary.tc.faa.gov) in Adobe Acrobat portable document format (PDF).

**Form DOT F 1700.7 (8-72)**

Reproduction of completed page authorized

1. Report No. <b>DOT/FAA/TC-20/21</b>	2. Government Accession No.	3. Recipient's Catalog No.	
4. Title and Subtitle <b>Post-Crash Fire Forensic Analysis on Aerospace Composites – Literature Review</b>		5. Report Date <b>August 2020</b>	
		6. Performing Organization Code	
7. Author(s) <b>Hajar Righi, Abhijith Madabhushi, Hasnaa Ouidadi, Dounia Boushab, Thomas Lacy, Santanu Kundu, Charles Pittman, and Matthew W. Priddy</b>		8. Performing Organization Report No.	
9. Performing Organization Name and Address <b>Mississippi State University 479-1 Hardy Road Mississippi State, MS 39762</b>		10. Work Unit No. (TRAIS)	
		11. Contract or Grant No.	
12. Sponsoring Agency Name and Address <b>U.S. Department of Transportation Federal Aviation Administration Washington, DC 20591</b>		13. Type of Report and Period Covered <b>Final Report</b>	
		14. Sponsoring Agency Code <b>AIR-600</b>	
15. Supplementary Notes <b>The FAA Technical Monitor for this research was Dave Stanley at the FAA William J. Hughes Technical Center in Atlantic City, NJ.</b>			
16. Abstract <p>This report provides an initial literature review detailing the effects of fire on fiber-reinforced composites. This review summarizes the current state of experimental testing on composite materials with applications to commercial aircraft and ships. Additionally, this review includes fire damage mechanisms (i.e., matrix decomposition/pyrolysis, fibers ablation/sublimation, outgassing, delamination, and char formation) that occur when exposing a composite material to controlled open flame or heat fluxes. Non-destructive inspection (NDI) and destructive inspection techniques for assessing the severity and extent of fire damage were incorporated, along with modeling techniques used to predict progressive degradation in composite thermal and mechanical properties as a function of increasing temperature, heat flux, and exposure time. Physical char removal techniques (i.e., dry ice blasting) were studied and included in this literature review. Chemical, combined physical-chemical techniques and commercial cleaning solvents for removing char and other fire by-products were also reviewed.</p>			
17. Key Words <b>Fire damage, char removal, composite materials, fiber-reinforced composites</b>		18. Distribution Statement <b>This document is available to the U.S. public through the National Technical Information Service (NTIS), Springfield, Virginia 22161. This document is also available from the Federal Aviation Administration William J. Hughes Technical Center at <a href="http://actlibrary.tc.faa.gov">actlibrary.tc.faa.gov</a>.</b>	
19. Security Classif. (of this report) <b>Unclassified</b>	20. Security Classif. (of this page) <b>Unclassified</b>	21. No. of Pages <b>52</b>	22. Price

## **Contents**

<b>1</b>	<b>Introduction.....</b>	<b>1</b>
<b>2</b>	<b>Literature review .....</b>	<b>2</b>
2.1	Fire effects on composite materials.....	2
2.2	Surface characterization of composite materials.....	24
2.3	Surface characterization of thermally degraded composites.....	26
2.4	Char removal techniques .....	32
<b>3</b>	<b>Conclusion .....</b>	<b>36</b>
<b>4</b>	<b>References.....</b>	<b>37</b>

## Figures

Figure 1. Schematic of a vertical Bunsen burner draft-free test cabinet (Horner, 2000).....	4
Figure 2. Schematic of a horizontal Bunsen burner draft-free test cabinet (Horner, 2000) .....	5
Figure 3. Test setup for (a) vertical and (b) horizontal burn tests (Horner, 2000).....	6
Figure 4. Illustration for the use of the flame indicator prongs (Horner, 2000) .....	7
Figure 5. The FAA NextGen burner (Johnston et al., 2000) .....	8
Figure 6. Side view of a buckled CFRP sample after ten minutes of fire exposure (Hode, 2012). 9	
Figure 7. Kerosene-fired FAA NextGen burner and sample frame (Hode, 2012) .....	9
Figure 8. Front view of CFRP sample after ten minutes of fire exposure (Hode, 2012).....	10
Figure 9. Fire effects on a carbon/epoxy composite material (Gillian et al., 2017) .....	11
Figure 10. Fire-progress as a function of temperature for fiberglass laminate (Puchades, 2016) 13	
Figure 11. Relative mass-loss% vs. temperature (Cytec 977-3 at 20 °C/min in N <sub>2</sub> and air) (Brown, A et al., 2012) .....	14
Figure 12. GFRP/balsa sandwich panel exposed to a heat flux of 50 kW/m <sup>2</sup> (Puchades, 2016) .	15
Figure 13. Temperature-time profile at the regions exposed to 50 kW/m <sup>2</sup> heat flux (Anjang et al., 2014) .....	15
Figure 14. Fire-degraded fibers in an AS4/3501 laminate (780x) (Greenhalgh, 2009).....	16
Figure 15. Cone calorimeter (Brown, A et al., 2015) .....	17
Figure 16. Schematic of the large-scale fire test (Mouritz et al., 2001) .....	18
Figure 17. Measured temperatures in the cone calorimeter and fuel fire tests on GRP panels (Mouritz et al., 2001) .....	18
Figure 18. (a) Through-thickness fire damage, (b) char-layer, (c) delamination cracks SEM (Mouritz et al., 2001) .....	19
Figure 19. A cross-sectional view of an 11.5 mm thick non-coated composite after burning (Mouritz & Mathys, 2001).....	20
Figure 20. (a) fire damage schematic, (b), (c), (d), and (e) SEM micrographs (Mouritz & Mathys, 2001) .....	21
Figure 21. Cross-section view of the carbon/epoxy composite after a fire test (Mouritz, 2003) .	22
Figure 22. Fire effects on post-fire char thickness, flexural strength, and modulus (Mouritz, 2003) .....	23
Figure 23. Schematic of typical burn zones due to fire damage (Kiel, 2006) .....	24
Figure 24. Fracture analysis logic network (Walker, 1995) .....	26
Figure 25. SEM of cross-sections showing the effects of aging (Wolfrum et al., 2009).....	27

Figure 26. Micrographs showing surfaces of degraded samples at 1000 °C (Grange et al., 2018)	28
Figure 27. Micrographs of the crash specimens (a), (c) Before, (b),(d) After TGA (Tadini et al., 2017)	29
Figure 28. Micrographs of fiber-matrix interfaces showing thermal exposure (Liu et al., 2016)	30
Figure 29. (a),(b) Through thickness micrographs, (c),(d) Reaction mechanism schematics (Schuhler et al., 2018)	31
Figure 30. Ultrasonic C-Scans of carbon/PPS laminates in compressive loadings after fire (Maaroufi et al., 2017)	32
Figure 31. SEM images of the carbon fibers before and after recovery (Fernández et al., 2018)	33
Figure 32. Cold jet ice blasting steps (ColdJet)	35
Figure 33. Schematic showing the ultrasonication process (EpiSonic)	36
Figure 34. Flow diagram showing the physics of ultrasonication	36

## **Tables**

Table 1. List of chemical solvents and commercially available products for char removal.....	34
--	----

## Acronyms

Acronym	Definition
AC	Advisory Circular
CFRP	Carbon Fiber Reinforced Polymer
FAA	Federal Aviation Administration
GFRP	Glass Fiber Reinforced Polymer
GRP	Glass Fiber Reinforced Polyester
ILS	Interlaminar Shear
IPS	In-Plane Shear
NDI	Non-Destructive Inspection
PEKK	Polyetherketoneketone
PPS	Polyphenylene Sulfide
SEM	Scanning Electron Microscope
TGA	Thermogravimetric Analysis



## Executive summary

Composite aircraft structures subjected to failure during accidents are often subjected to post-crash fire. The resulting fire damage often changes the failure surfaces—making it more difficult to identify the root cause of structural failure. Therefore, there arises a need for the development of an effective fire-damage assessment methodology to perform fire forensics on the burned aircraft structural elements and assess the effect of fire damage on the fracture surfaces developed during mechanical failure.

The current project aims to accomplish the following:

- i. Compare current thermoset composite specimens systems subjected to various mechanical failure modes against to the failure characteristics outlined in the existing Composite Failure Analysis Handbook developed by the FAA and the Air Force Research Lab (AFRL).
- ii. Develop a test protocol for burning small-scale carbon/graphite reinforced epoxy specimens and identify the salient fire damage characteristics (i.e., melt dripping, char, and soot deposition).
- iii. Develop a test protocol for removing the fire damage remnants (char and soot, melt dripping).
- iv. Characterize and identify the salient features of composite surface (pristine and mechanically failed) before and after char removal.

The teams at Mississippi State University (MSU) and Texas A&M University (TAMU) performed an initial literature survey to help execute the project objectives.

This document summarizes the current state of research on the effects of fire on fiber-reinforced composites. This review also details the experimental testing on composite materials with applications to commercial aircraft and ships. Fire damage mechanisms (i.e., matrix decomposition/pyrolysis, fibers ablation/sublimation, outgassing, delamination, and char formation) that occur when exposing a composite material to controlled open flame or heat fluxes were reviewed. Non-destructive inspection (NDI) and destructive inspection techniques for assessing the severity and extent of fire damage are also incorporated. Physical char removal techniques (i.e., dry ice blasting) were studied and included in this literature review. Chemical-based, combined physical-chemical techniques and commercial cleaning solvents for removing char and other fire by-products were also reviewed. This review also catalogs the research in the modeling of composite materials response to fire propagation. Modelling techniques used to

predict progressive degradation in composite thermal and mechanical properties as a function of increasing temperature, heat flux, and time exposed to the fire were also reviewed.

The literature survey is part of the ongoing research efforts at MSU and TAMU in developing a test protocol for performing fire forensics on aerospace composite structural elements. The end goal of this research is to incorporate a fully developed fire forensics protocol that is compatible with prominent aerospace composite material systems into the composite failure analysis handbook.

# 1 Introduction

Fiber-reinforced composite materials are increasingly used as an alternative to metals in commercial aircraft, general aviation (GA) aircraft, and unmanned aerial system primary structures because of their relatively high strength-to-weight and stiffness-to-weight ratios, excellent corrosion resistance, and complex design capabilities (Kabche, 2006; Botelho et al., 2006; Phil & Soutis, 2014; FAA, 2018; Mouritz & Gibson, 2007; Mouritz, 2003; Guimarães et al., 2020). In general, damage tolerance assessments of laminated composites and sandwich structures are much more complicated than for metallic structures because of the composites' *i*) heterogeneous structure, *ii*) greater strain-rate and temperature dependence, *iii*) multitude of disparate failure mechanisms (matrix cracking, fiber-matrix debonding, delamination, fiber rupture, fiber micro-buckling, face sheet crimping and delamination buckling, core instability, and *iv*) potential degradation in extreme environments (Kabche, 2006; Botelho et al., 2006; Caccese et al., 2004; Rouchon, May 2009; Sun et al., 2002; Alderliesten, 2015). Exposure to extreme environments can also severely degrade aircraft flight safety, damage tolerance, and structural integrity (Mouritz & Gibson, 2007; Mouritz, 2003).

Prolonged fire exposure—whether in-flight or on the ground—may result in severe degradation in composite material performance and reductions in overall flight safety (Greenhalgh, 2009; Wright et al., 2003). Locally high temperatures (below the resin curing temperature) cause a decrease in composite elastic moduli due to matrix softening, increasing the likelihood of thermal stability or matrix-dominated failures. As the temperature exceeds the resin curing temperature, thermosetting matrices will further cure, decompose, and then ignite. Matrix burning may lead to toxic smoke and progressive char formation (Mouritz & Gibson, 2007). At extreme temperatures, carbon fiber fragmentation, sublime, and ablation can occur (Greenhalgh, 2009). Large-scale matrix decomposition and combustion, surface char formation, and high-temperature gradients may cause substantial mechanical damage to the underlying composite, resulting in significant decreases in moduli and strengths (Mouritz & Gibson, 2007; Mouritz, 2003; Chen, 2018; Mouritz & Mathys, 2001; Mouritz et al., 2001). Moreover, char formation and other thermal by-products, due to post-crash fires, can mask relevant aspects of the structural damage morphology and other evidence necessary to identify the underlying failure mechanisms, which caused catastrophic structural failures (Horner, 2000).

Fire-resistance of composite materials can be improved by adding fire retardants to the matrix or using a thermal barrier coating to reduce flammability and mitigate the effects of fire on the mechanical properties (Mouritz & Gibson, 2007). However, using such compounds results in toxic, corrosive gas content and other carcinogenic substances during combustion (Majlingová

& Jinb, 2018; Ray & Kuruma, 2019). Intumescent coatings can also be inefficient for certain materials, with leeching occurring in some cases (Popescu & Pfriem, 2020). The char produced from the combustion of fire-retardants is porous and reduces structural integrity (Camino et al., 1989). Moreover, the presence of an adherent char layer is not conducive to fractography. Therefore, removing char from the fire-exposed composite surface is important to deduce the root cause of the fire and identify the underlying failure mechanisms (Sarkos, 2011; Chen, 2018; Kar et. al, 1993; Walker, 1995; Kar, 1992).

## 2 Literature review

### 2.1 Fire effects on composite materials

Unlike traditional metallic airframe materials, many aerospace composite materials are combustible and prone to smoldering and re-ignition after an initial fire is extinguished (Wright et al., 2003). Hence, aerospace composite structures' fire endurance and fire resistance may be profoundly different from metallic structures (Zhuguo et al., 2011). Direct exposure or indirect exposure can result in severe damage to conventional aircraft composite structures. Fire endurance and fire effects on composite materials are interrelated because they follow similar testing procedures. A brief overview is presented for fire endurance followed by specifics related to the effects of fire on composite materials.

According to the Federal Aviation Administration (FAA) Advisory Circular (AC) 20-135, a fire test designed to quantify fire resistance of an aircraft composite should apply a flame that can produce a temperature of  $1093 \pm 83$  °C ( $2000 \pm 150$  °F), and should be 6.4 mm (0.25 in) above the sample's surface while maintaining a heat flux density of  $105.6 \text{ kW/m}^2$  ( $9.3 \text{ BTU/ft}^2\text{-second}$ ) over an area of approximately 12.5 cm x 12.5 cm (5 in x 5 in).

The fire resistance of a composite can be improved by coating with fire-resistant materials (Mouritz, 2002). For example, thermal barrier materials (i.e., ceramic fiber blankets or intumescent mats) have shown the ability to delay the combustion process (Mouritz, 2002). The use of resins with fire-retardant additives (i.e., aluminum trihydrate, antimony trioxide, or zinc borate) is also a common technique developed to improve the fire resistance of composite materials.

Most composite materials soften and creep at low temperatures (100-200 °C), leading to an increased likelihood of buckling or stability related failures (Mouritz & Gibson, 2007). Once the local temperature exceeds 300-400 °C, epoxy matrices will further polymerize and decompose. Once the matrix reaches its ignition temperature ( $>400$  °C for epoxy), it will burn, resulting in

the production of volatiles and progressive char formation (Mouritz & Gibson, 2007). At extreme temperatures ( $>3000\text{ }^{\circ}\text{C}$ ), the carbon fibers can longitudinally split/fragment, sublime, and ablate (Greenhalgh, 2009). Such fire damage can result in significant mass loss (Tranchard et al., 2015). Large-scale matrix decomposition/combustion, surface char formation, and high-temperature gradients can also lead to matrix cracking, delamination, and other damage to the underlying composite (Mouritz, 2002; Chen, 2018; Mouritz & Mathys, 2001).

Large-scale aircraft composite structures subjected to external fuel-fed fires may collapse due to local reductions in the mechanical properties (Zhuguo et al., 2011). Also, the ignition of fuel vapors can over-pressurize composite fuel tanks, resulting in a catastrophic failure of primary load-bearing aircraft structures (Zhuguo et al., 2011). Due to these potential failures, the FAA imposed additional requirements on the composite parts of the Boeing 787 (fuselage, wings, fuel tank skins). FAA AC 20-107B requires establishing testing protocols and analysis procedures for evaluating the structural integrity of composites exposed to fire once the temperature exceeds maximum operating conditions.

The fire resistance and endurance of a given composite structure depend on the material system, layup, structural geometry, fire duration, fire intensity, and structural loading. Since matrix decomposition, char, and other damage due to post-crash fires can mask critical elements of structural damage morphology, special care should be taken when identifying critical structural failure mechanisms that led to catastrophic crashes preceding a fire.

Vertical and horizontal Bunsen burner test protocols were defined by the FAA in the aircraft materials fire-test handbook, entitled DOT/FAA/AR-00/12 (Horner, 2000), to address the tests specified in Title 14, Code of Federal Regulations (14 CFR) §25.853 and §25.855 for determining the fire resistance of aircraft cabin and cargo compartment materials. These protocols include 12 s and 60 s vertical Bunsen burner tests and a 15 s horizontal Bunsen burner test (Horner, 2000). A minimum of three samples is required for each burn test according to the defined protocols.

A specimen size of at most  $3 \times 12 \times 1\text{ in}^3$  ( $W \times L \times T$ ) was adopted for both the vertical and horizontal burn tests as a means to produce repeatable levels of char across multiple specimens. Before the burn test, the specimens should be conditioned at  $70^{\circ} \pm 5\text{ }^{\circ}\text{F}$  temperature and  $50\% \pm 5\%$  relative humidity for a minimum of 24 hours. All burn tests should be performed in a draft-free cabinet located inside an exhaust hood. The schematics for the cabinet designs used in the burn tests are shown in Figure 1 and Figure 2. Figure 3 and Figure 4 show the vertical and horizontal orientations of the specimens. During the fire test, a Bunsen burner is placed at the edge of the specimen beneath the midpoint of its cross-section while maintaining a distance of

0.75 in between the top of the burner and the specimen edge. During the test, ignition time, flame time, drip flame time, and burn length should be recorded for each specimen (Horner, 2000).

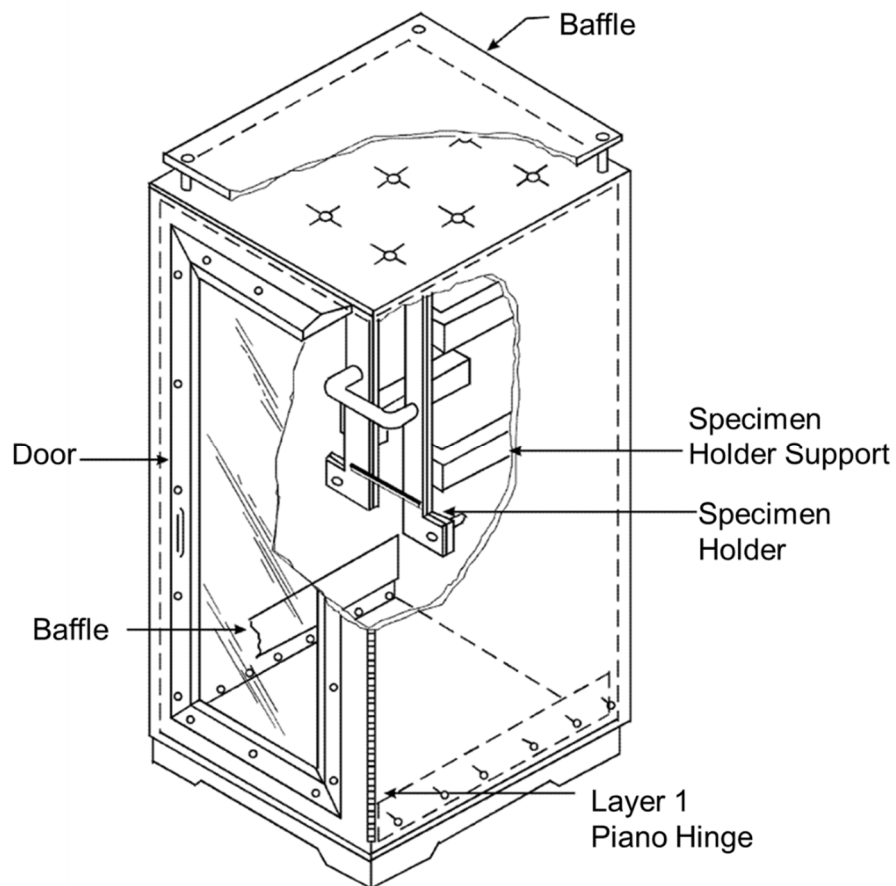


Figure 1. Schematic of a vertical Bunsen burner draft-free test cabinet (Horner, 2000)

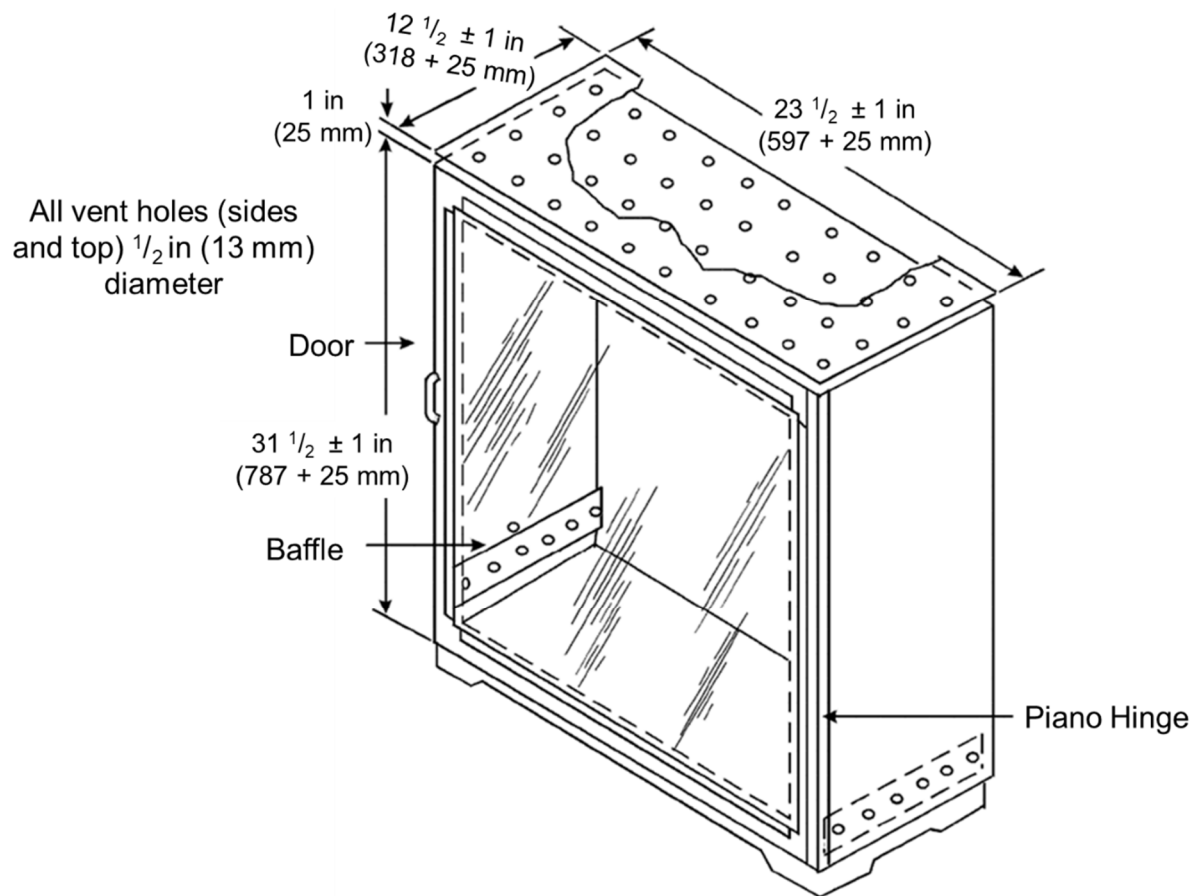


Figure 2. Schematic of a horizontal Bunsen burner draft-free test cabinet (Horner, 2000)

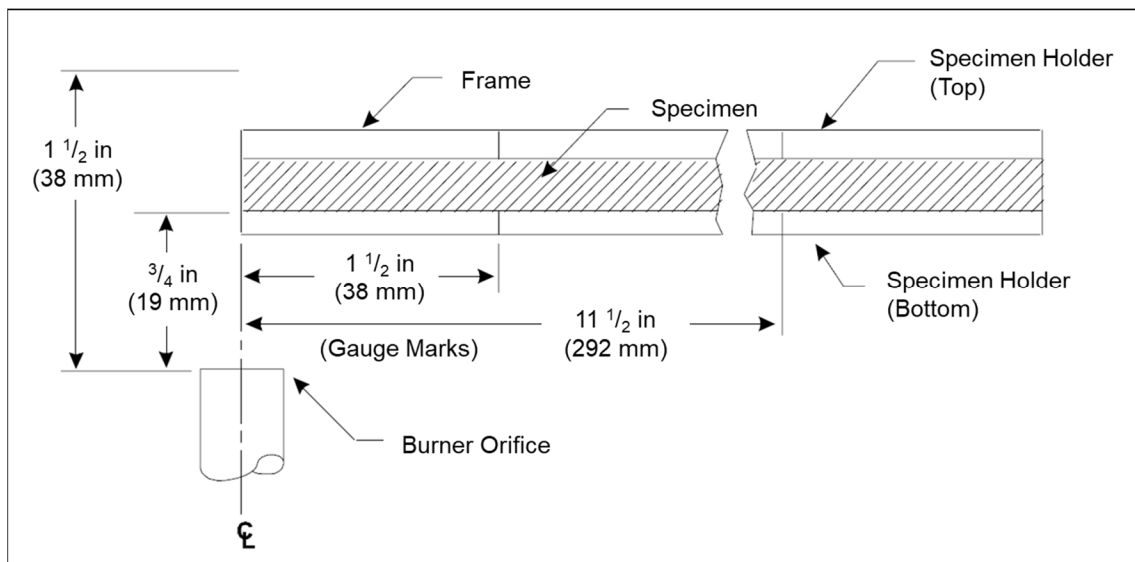
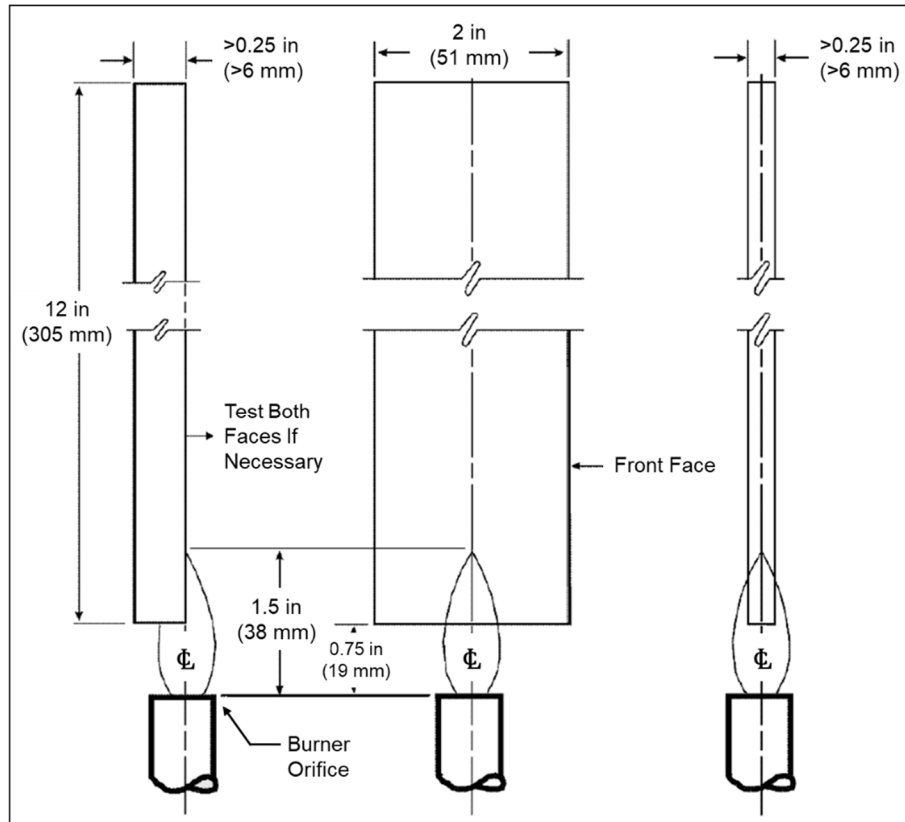


Figure 3. Test setup for (a) vertical and (b) horizontal burn tests (Horner, 2000)



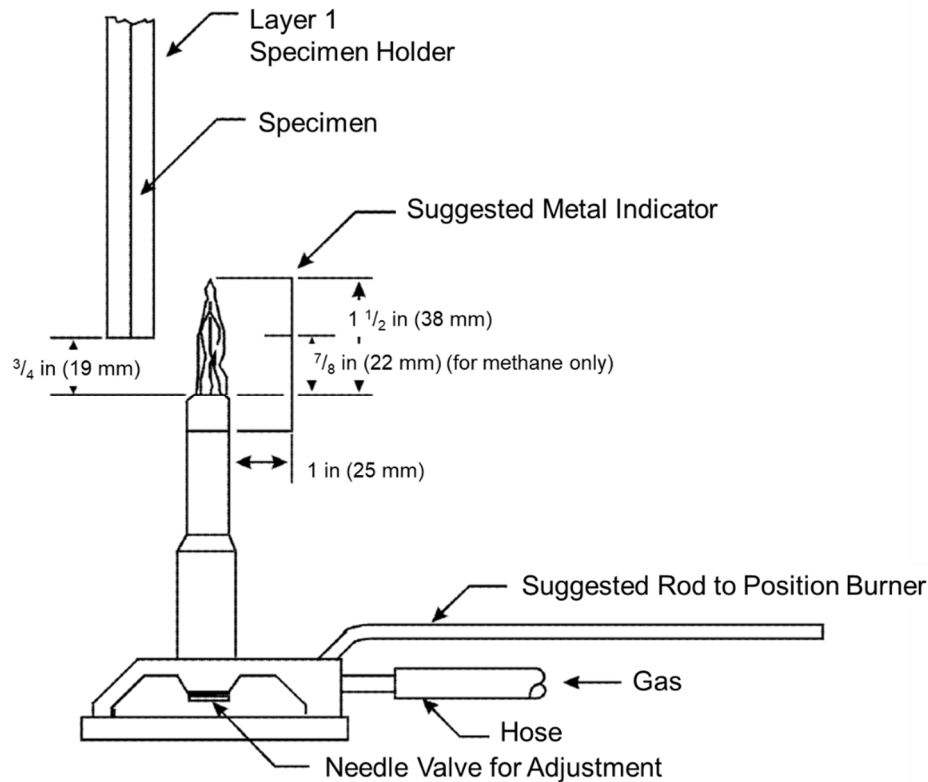


Figure 4. Illustration for the use of the flame indicator prongs (Horner, 2000)

Sandia National Laboratories conducted a literature review examining the decomposition behavior of carbon/epoxy composites subjected to fire (Brown, A, 2013). The effects of binder reactions, fiber decomposition, heat transfer, pyrolysis products, scale effects, swelling, burn-through, combined thermal/structural effects, ignition, and health effects were considered. The study concluded that most fire performance data available in the literature involved length/mass scales that were orders of magnitude below those commonly employed in practical vehicle designs. Full-scale fuel-fed direct fire experiments are challenging to perform. The FAA, therefore, developed a "NextGen" gun-type burn-through test method shown in Figure 5 to reliably simulate open-pool fuel fires for large-scale specimens at flame temperatures up to 1038 °C (Ochs & Hode, 2009).

The FAA NextGen Burner laboratory is one of the few facilities capable of performing direct fire endurance tests on large structures (Hode, 2012). To simulate severe fire conditions, the FAA developed and adopted multiple oil burners to test aircraft materials and systems. The goal was to provide a burner with a simple design, operation, and maintenance. The updated NextGen burner (Figure 5) is currently being used mostly for power plant, cargo liner, seat cushion, and thermal, acoustic insulation burn-through testing (Ochs, 2010). This burner can generate temperatures over 990 °C, similar to a fuel-fed pool fire scenario (Hode, 2012).

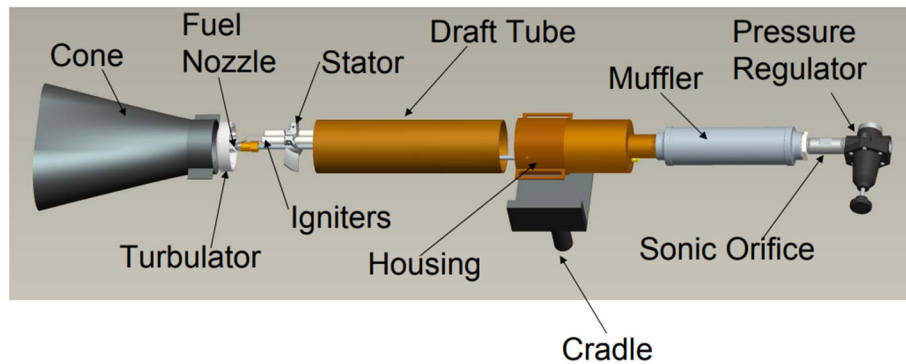


Figure 5. The FAA NextGen burner (Johnston et al., 2000)

The FAA performed 20 tests on carbon fiber composite samples using the NextGen Fire burner mounted at a 45° angle on glass laminate aluminum reinforced epoxy (GLARE) and carbon-fiber-reinforced polymer (CFRP) (Hode, 2012). The deformed configuration of the specimens and the experimental setup are shown below (see Figure 6, Figure 7, and Figure 8). Out of the 20 samples tested, 7 buckled at 23 to 42 seconds once the test started (Hode, 2012), as shown in Figure 6 and Figure 8 (Hode, 2012). Fire-induced internal matrix pyrolysis produces internal pressurized gases that lead to void formation/cavitation and swelling. Resin bubbles were visible at the border of the damaged areas. Smoke appeared roughly 16 seconds after the beginning of the tests. A reduction in smoke typically occurred before mechanical failure. For all 20 tests, flaming continued for 1-3 minutes after extinguishing the NextGen burner. Fourteen samples exhibited smoldering, either immediately or up to 2.55 minutes after exposure. This study showed that smoking, smoldering, and flaming combustion occurred to different degrees during and after fire exposure, depending on the exposure duration. The smoldering was only induced by the heating of the carbon fibers (Hode, 2012).



Figure 6. Side view of a buckled CFRP sample after ten minutes of fire exposure (Hode, 2012)



Figure 7. Kerosene-fired FAA NextGen burner and sample frame (Hode, 2012)



Figure 8. Front view of CFRP sample after ten minutes of fire exposure (Hode, 2012)

Inspired by the FAA NextGen burner, Tranchard developed a versatile kerosene-based fire burner (Tranchard et al., 2015). The fire behaviors of 4 mm thick autoclaved-cured unidirectional and quasi-isotropic carbon/epoxy laminates at a calibrated flame temperature of 1038 °C and heat flux of 182 kW/m<sup>2</sup> were observed. X-ray microtomographic imaging was used to examine composite post-fire damage morphology, including the degree of matrix cracking, thermally induced delamination cracking, and matrix thermal decomposition. Five different composite degradation steps were identified during the mass loss measurements. During the first stage (from 0-25 seconds of fire exposure), there was no change in the mass and color of the specimen. The second stage (from 25-75 seconds) was marked by the beginning of thermal degradation. During this stage, a variety of gases were released, and specimen mass loss occurred. Nitrous oxide (NO) was produced due to the degradation of the triglycidyl meta-aminophenol component of the resin, while sulfur monoxide (SO) results from the degradation of the hardener. Water (H<sub>2</sub>O) and carbon dioxide (CO<sub>2</sub>) are the combustion products of flammable pyrolysis gases and oxygen. In the third stage (from 75-130 seconds), the mass loss rate and released gas concentration increased. The flame intensity also increased due to the burning of the gases released by matrix decomposition. This resulted in a higher rate of matrix thermal degradation,

which caused the additional gas release. The peak concentration of released gases was noticed at the beginning of the fourth stage (from 130-300 seconds). The gaseous products resulting from the decomposition process permeated through the material to the non-exposed surface.

Immediately afterward, the mass loss rate and concentration of the released gases decreased. At the fifth stage (from 300-315 s), the flame was stopped, and the rate of mass loss and released gas concentration continued to decrease until terminating at around 315 seconds when the small flames self-extinguished.

Scanning electron microscope (SEM) observations were used to examine the burned surface. However, there appeared to be a dependency of the effective thermal conductivities based upon on the properties of the fiber and matrix, constituent volume fractions, and layup. Cases of delamination were noticed in both specimen configurations. However, the unidirectional laminates displayed less delamination than quasi-isotropic laminates. This suggests that the composite layup can play a crucial role in fire damage development (Tranchard et al., 2015).

When CFRP composites are exposed to high temperatures, the matrix decomposes, producing volatile gases (Chen, 2018). The combustion of those gases with oxygen produces smoke, heat release, carbon monoxide (CO), carbon dioxide (CO<sub>2</sub>), and carbonaceous solid char. Therefore, exposing the top surface of a carbon/epoxy composite laminate to fire results in matrix-decomposition/degradation. Figure 9 shows a schematic of the fire effects on a carbon/epoxy composite material when subjected to fire (Gillian et al., 2017). Matrix cracks and delamination occur in the underlying layers due to thermal stresses and outgassing (Chen, 2018).

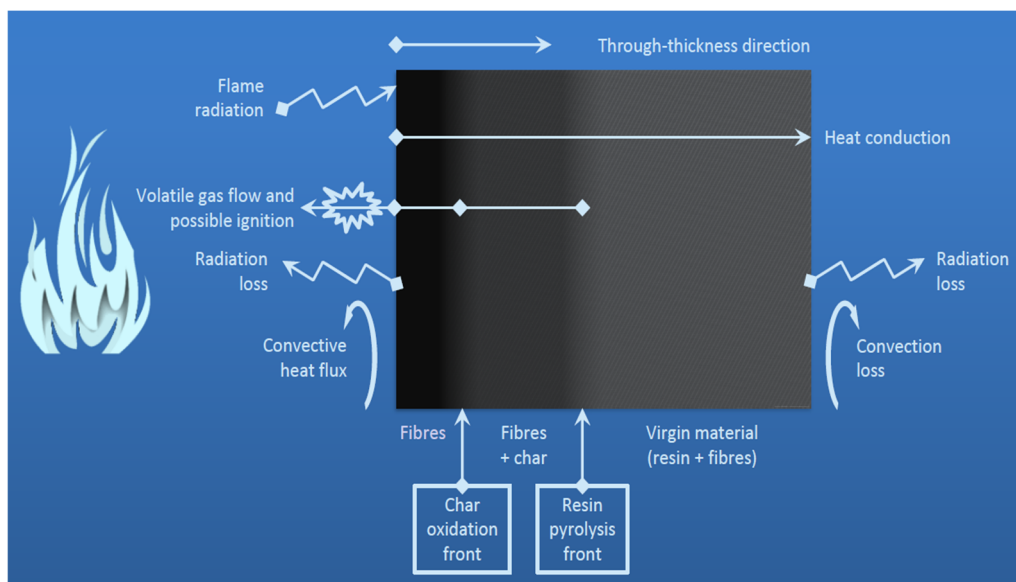


Figure 9. Fire effects on a carbon/epoxy composite material (Gillian et al., 2017)

Brown (Brown, A, 2013) investigated the swelling propensity of carbon fiber epoxy laminates when exposed to fire. The char deposited on the fire exposed surface, and the fibers prevent the release of the internal gases (i.e., epoxy matrix pyrolysis), causing internal pressurization and cavitation/porosity formation. This results in composite blistering, delamination, and swelling that can cause an average laminate thickness increase of 100-200%. The internal gas zone formed also slows down the heat conduction between plies. For coupons with smaller in-plane dimensions ( $<10$  cm), combustible gases escape the laminate edges, causing swelling. Whereas for bigger coupons ( $\geq 10$  cm), only the center of one laminate surface is exposed to fire. The unexposed areas with lower temperatures do not allow the combustible gases to escape through the laminate edges. For these specimens, swelling is limited to the composite area surrounding the flame's center. The combustion-induced gases typically follow an escape pathway depending on the burn location and its proximity to the composite edges (Brown, A, 2013).

When carbon fiber-reinforced epoxy laminates are exposed to fire, the following phenomena occur:

- Anisotropic heat conduction
- Thermal-induced deformation
- Decomposition of the polymer matrix and organic fibers
- Pressure rise due to formation of combustion gases and vaporization of moisture
- The flow of gases through the char zone
- Formation of delamination and matrix cracks
- Reactions between char and fiber reinforcement and ablation (Puchades, 2016; Kumar et al., 2018; Hubbard et al., 2011) (see Figure 10 (Puchades, 2016)).

During fire exposure, the char and decomposition regions expand to the non-exposed areas and increase the material's thickness (Kumar et al., 2018). Char formation begins at a pyrolysis temperature (250 °C to 600 °C) (Torre et al., 2000). The charred epoxy forms on top of the carbon fibers (Brown, A et al., 2012). Once the epoxy matrix is completely charred, the oxidation of carbon fibers begins (Kumar et al., 2018; Brown, A et al., 2012).



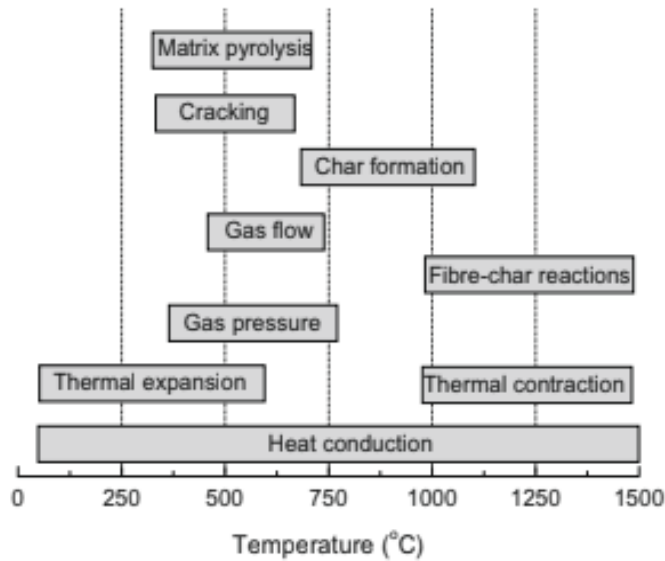


Figure 10. Fire-progress as a function of temperature for fiberglass laminate (Puchades, 2016)

Brown (Brown, A et al., 2012) also explored the bulk decomposition behavior of carbon/epoxy composites in severe fire conditions. Thermogravimetric analysis (TGA) experiments were performed on unidirectional Cytec 977-3 specimens. The single-ply specimens were heated in open 10 mm diameter platinum sample pans at a heating rate of 20 °C/min. Figure 11 shows the relative mass loss percentage vs. temperature for the Cytec 977-3 tested in an inert gas (nitrogen) and air (Brown, A et al., 2012). At approximately 280 °C, the epoxy begins to decompose slowly in both environments. The epoxy decomposition occurs over the temperature range of 300-500 °C (Puchades, 2016). Oxygen interaction plays an essential role in this phase, enhancing char formation and delaying the release of the pyrolysis gases (Brown, A et al., 2012; Brown, A. L. et al., 2011). As the temperature exceeds 500 °C, the fiber and matrix degrade to a porous carbonaceous char. The rapid oxidation of the remaining charred epoxy and carbon fibers occurs when the temperature reaches 650-700 °C. When the temperature exceeds 1000 °C, a significant char is formed, resulting in a considerable mass loss (Puchades, 2016). Heat conduction primarily occurs along the burned surface rather than through the material due to the relatively low thermal conductivity of the charred surface (Kumar et al., 2018). As an aside, Florio (Florio Jr et al., 1991) performed microscopy studies and observed that the presence of pores phenolic matrix composites would lead to entrapment of the decomposition gases within the polymer matrix, leading to pore-growth and coalescence. Consequently, the local pressure increases to a value 15 times greater than the ambient pressure, causing delamination, matrix cracking, and fiber-matrix debonding (Florio Jr et al., 1991).

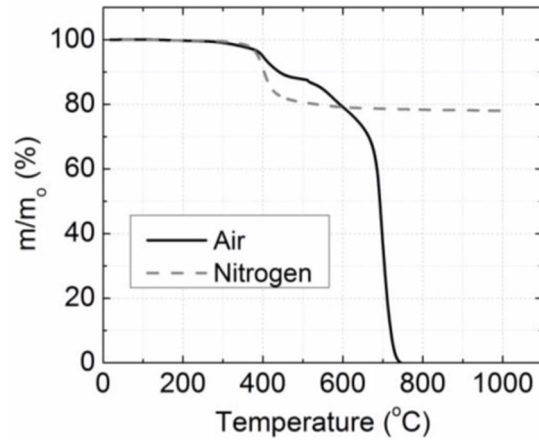


Figure 11. Relative mass-loss% vs. temperature (Cytec 977-3 at 20 °C/min in N<sub>2</sub> and air) (Brown, A et al., 2012)

Puchades (Puchades, 2016) studied the behavior of glass-fiber reinforced polymer (GFRP) face sheet/balsa-core composite sandwich panels at high temperatures. Figure 12 shows an image of a GFRP/balsa sandwich panel exposed to a heat flux of 50 kW/m<sup>2</sup> (Puchades, 2016). A char layer was formed on the sandwich composite facesheet when exposed to this heat flux. This char layer acted as a thermal barrier to prevent oxygen transfer between the atmosphere, and the unburnt interior of the composite, providing resistance to flame propagation throughout the material (Puchades, 2016; Hubbard et al., 2011). Most of the matrix (a vinyl-ester polymer) was decomposed into volatile gases, while only 5-10% of the original mass was converted into char (Puchades, 2016). In general, the charred layer has negligible mechanical properties. In addition, sandwich composites are well known thermal insulators. Anjang (Anjang et al., 2014) developed a thermal model that was capable of approximating the temperature profile of the Balsa core, front and back facesheets in GFRP facesheet/balsa-core composite sandwich panels exposed to a heat flux of 50 kW/m<sup>2</sup> for a maximum exposure time of 1800 s, as shown in Figure 13 (Anjang et al., 2014). The low thermal conductivity of the core material effectively insulates the two facesheets from one another (Anjang et al., 2014).



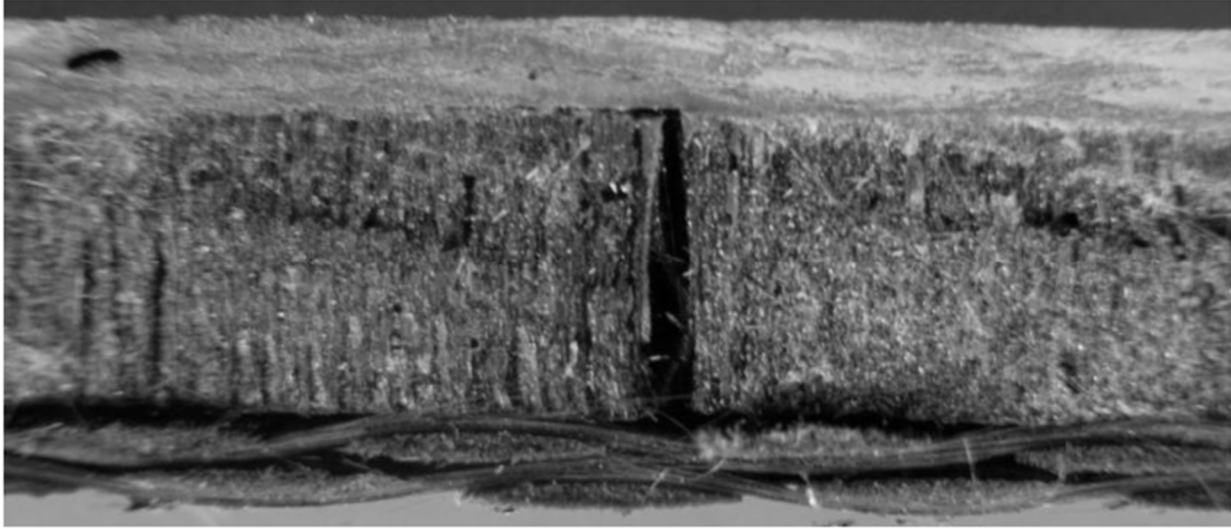


Figure 12. GFRP/balsa sandwich panel exposed to a heat flux of 50 kW/m<sup>2</sup> (Puchades, 2016)

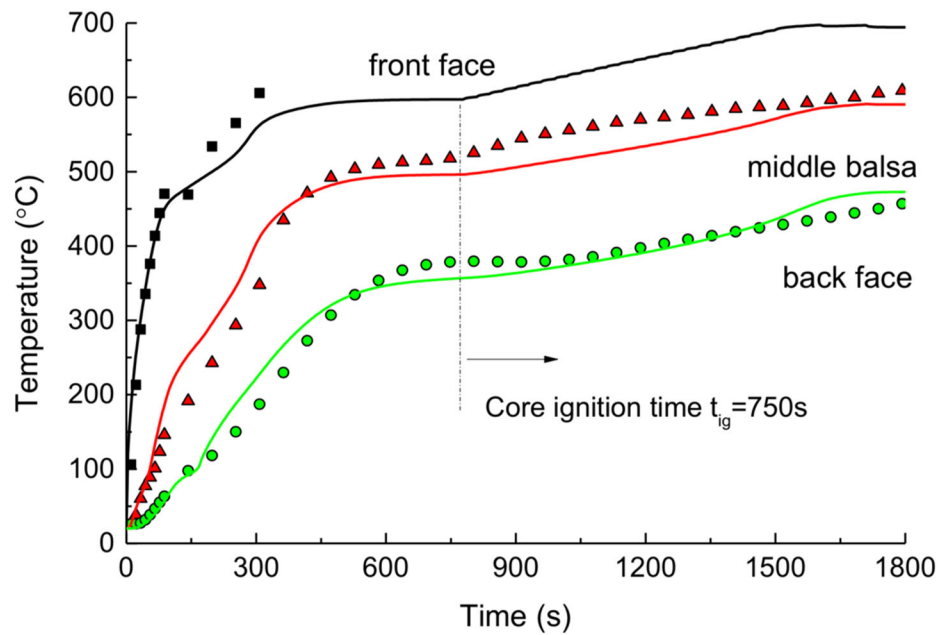


Figure 13. Temperature-time profile at the regions exposed to 50 kW/m<sup>2</sup> heat flux (Anjang et al., 2014)

When fiber-reinforced polymer composites are exposed to fire, the polymeric matrix will embrittle and char, leaving a sooty deposit that can act as a thermal barrier. This can serve to protect the underlying composite. The matrix may completely decompose/disintegrate after intense fire exposure, leaving only the remnants of carbon or glass fibers (aramid fibers will tend to vaporize fully) (Greenhalgh, 2009). Exposed carbon fibers may oxidize, longitudinally split,

fragment along their lengths, and become partially aerosolized. This adversely affects the structural integrity of the composite. Figure 14 shows a micrograph of fire-degraded fibers in an AS4/3501 carbon/epoxy laminate (Greenhalgh, 2009).

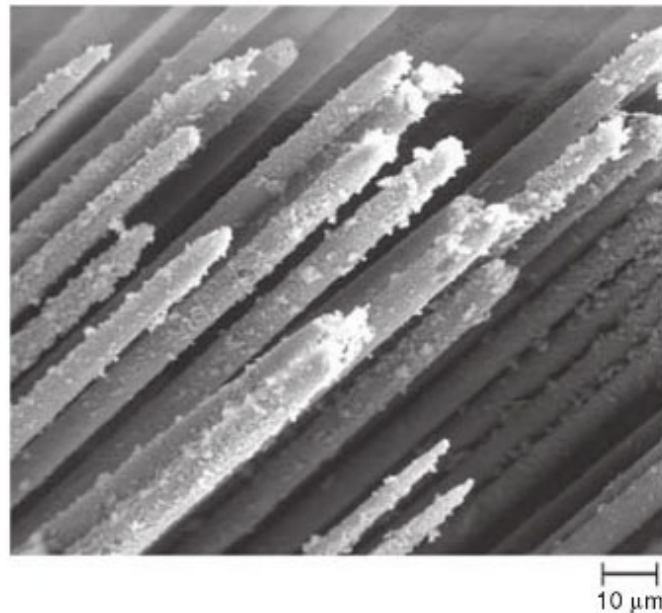


Figure 14. Fire-degraded fibers in an AS4/3501 laminate (780x) (Greenhalgh, 2009)

Inexpensive cone calorimeter tests can be performed using small samples to assess the samples' ignition time, mass loss, heat release rate, smoke production, and chemical composition of fumes emitted for a given heat flux (i.e., indirect fire exposure). A cone calorimeter (shown schematically in Figure 15) utilizes an oxygen-depletion calorimetry measurement method (Mouritz & Gardiner, 2002). The oxygen consumed during the burning process is directly proportional to the heat released at combustion. Properties of composites exposed to fire vary depending on the constituents, fire conditions, and the test method (Mouritz, 2006).

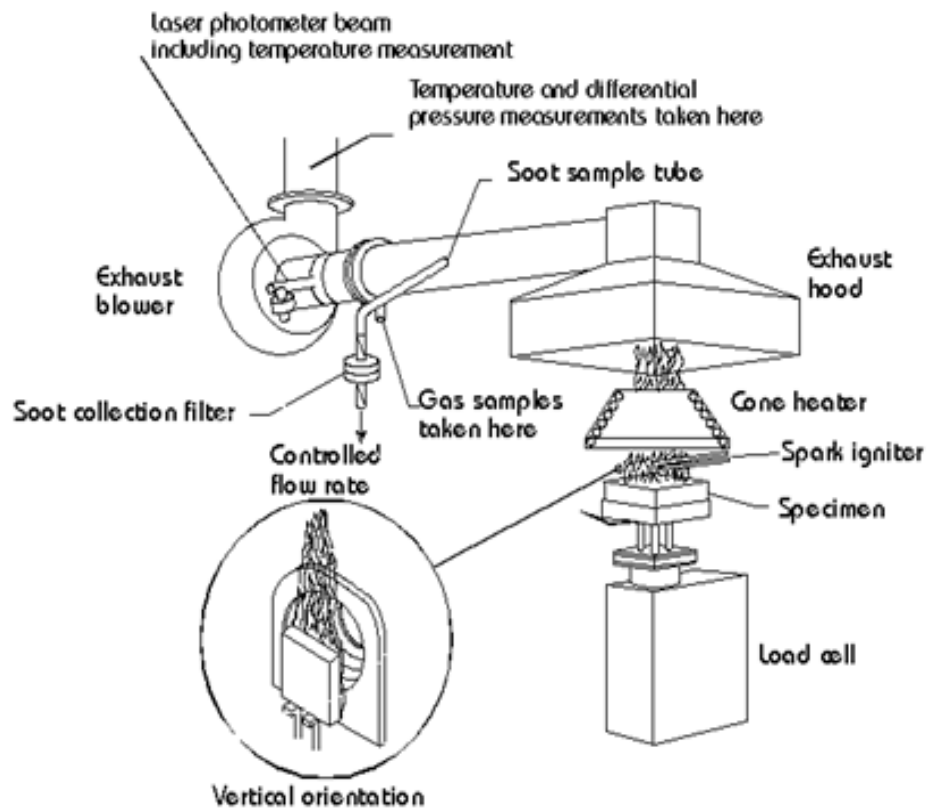


Figure 15. Cone calorimeter (Brown, A et al., 2015)

Mouritz (Mouritz et al., 2001) conducted a set of experiments to measure the mechanical properties of a Glass fiber reinforced polyester (GRP) laminate when subjected to an artificial fire inside a cone calorimeter and an actual large-scale kerosene pool fire (see Figure 16). This study aimed to investigate the use of low-cost, small-scale artificial fire tests to estimate the properties of composites exposed to large-scale real fire scenarios. A comparison of the thermal environment, ignition mechanics, fire damage processes, burn-through rates, and post-fire mechanical properties of the GRP composites obtained from calorimeter and kerosene fire tests were performed.

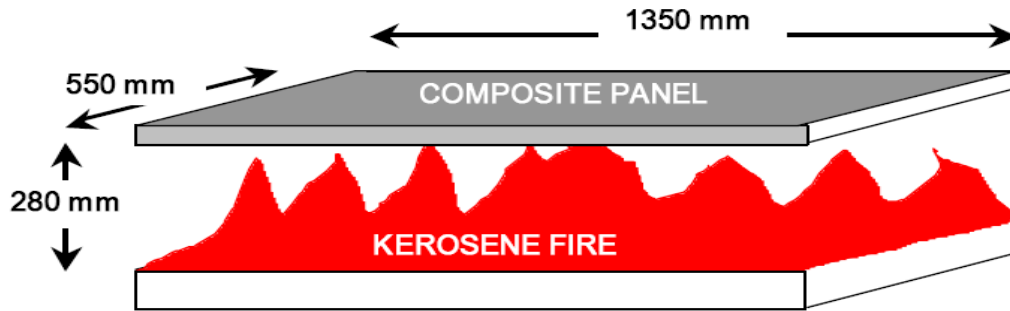


Figure 16. Schematic of the large-scale fire test (Mouritz et al., 2001)

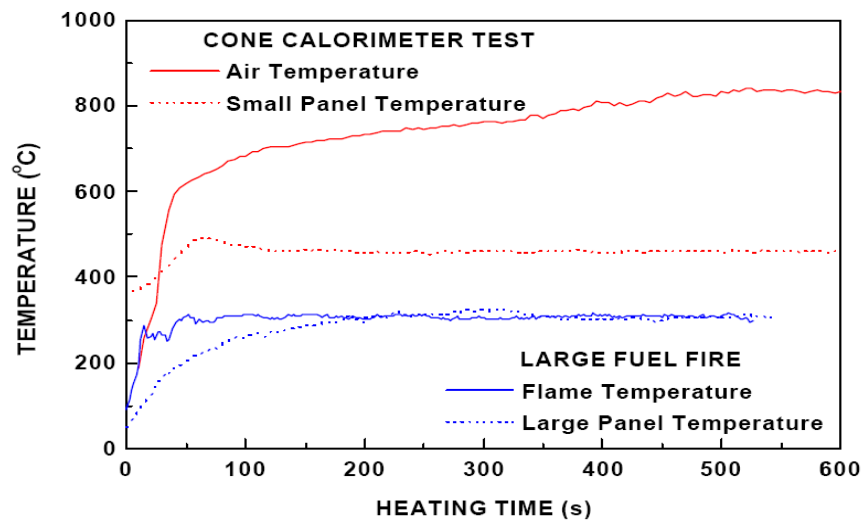


Figure 17. Measured temperatures in the cone calorimeter and fuel fire tests on GRP panels (Mouritz et al., 2001)

The fire damage induced on the small and large panels was investigated using SEM. The crack depths in the panels caused by the fire were determined using pulse-echo ultrasonics. The identified fire damage on the composite surfaces after the cone calorimeter and fuel fire testing is shown in Figure 18 (Mouritz et al., 2001). In both cases, the damage was nearly identical. Char formation started on the surface fibers in both small and large composite panels due to the combustion and thermal degradation of the polyester matrix upon ignition. Delamination occurred at the interphase between the burnt and unburnt parts of both small and large composite panels due to thermal strains produced during the burning. As the temperatures generated in the calorimeter were higher than those in the fuel fire tests, the charring, cracking, and burn-through rate for the small samples was higher than those for the large panel (Mouritz et al., 2001). The post-fire flexural stiffness and strength of the composite specimens were measured by quenching the burnt small and large panels and cooling them to room temperature. After cooling, the panels were cut into coupons with dimensions 240 mm long, 25 mm wide, and 12 mm thick. The

samples for cone calorimeter tests were thicker (13.5 mm) than those for fuel fire tests (12 mm). The burned part of the coupons was loaded to failure under bending-induced compression (Mouritz et al., 2001)

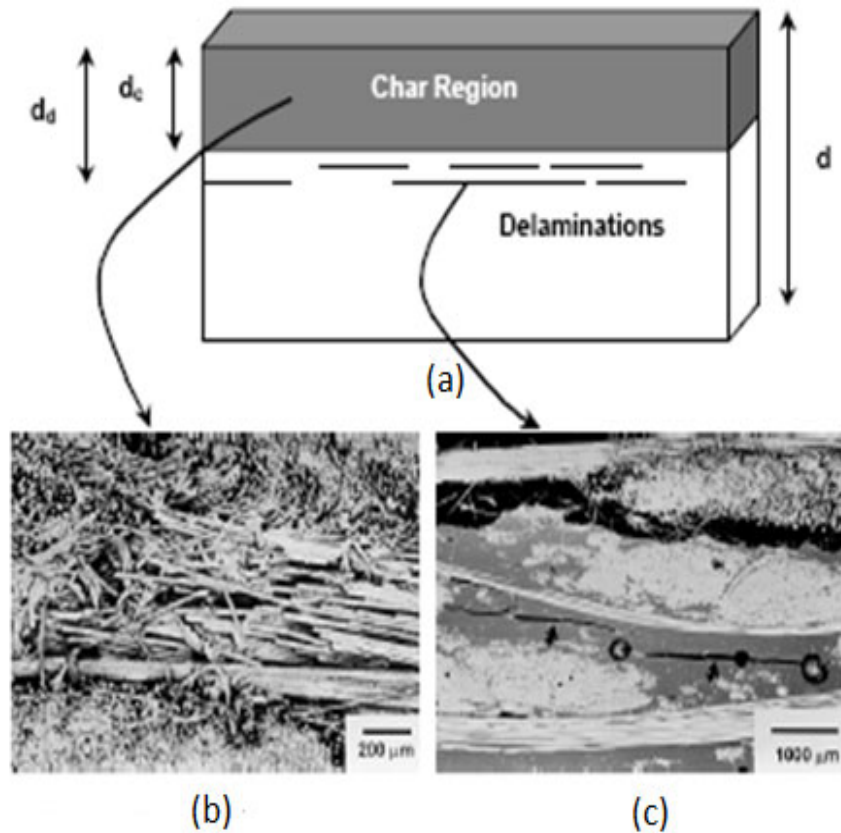


Figure 18. (a) Through-thickness fire damage, (b) char-layer, (c) delamination cracks SEM (Mouritz et al., 2001)

The cross-section of an 11.5 mm thick non-coated composite after being exposed to a heat flux of  $50 \text{ kW/m}^2$  at four different times (0, 85, 325, and 1800 s) is shown in Figure 19 (Mouritz & Mathys, 2001). Figure 19(a) represents the pristine composite. When exposed to fire, the outer layers of the composite started to char (black layer in Figure 19(b)). The char-thickness increased with exposure time (Figure 19(c)). Although the tested composite was 11.5 mm thick, the char spread through the whole thickness (Figure 19(d)) due to the polyester matrix's total thermal decomposition and combustion. Mouritz and Mathys (Mouritz & Mathys, 2001) also stated that the degree of char formation was independent of the heat flux, as the polyester matrix exothermally decomposed, producing heat that enhanced the combustion process upon the ignition of the composite. However, the char growth depended on the post-ignition heat-exposure time and oxygen transfer-rate to the combustion front. The combustion front is defined as the

interface between the burnt and unburnt layers of the composite. The oxygen transport rate dropped as the char thickness increased (Mouritz & Mathys, 2001).

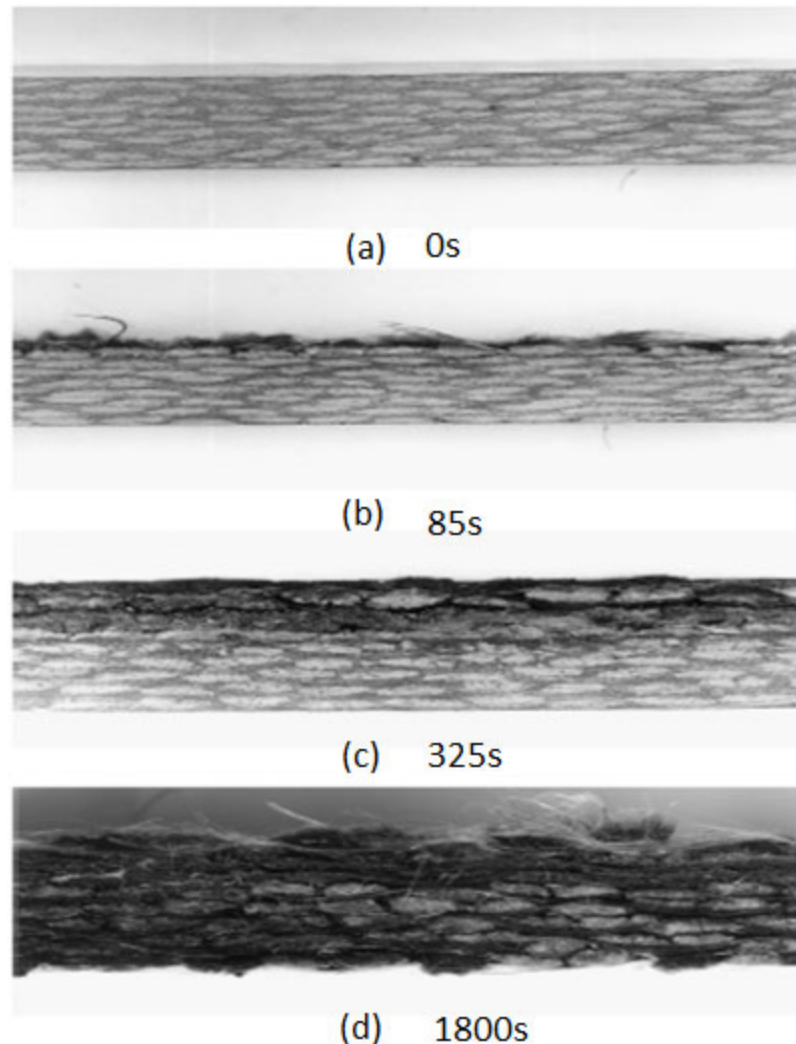


Figure 19. A cross-sectional view of an 11.5 mm thick non-coated composite after burning (Mouritz & Mathys, 2001)

Damage in the burnt coupons was assessed using SEM (see Figure 20 from (Mouritz & Mathys, 2001)). Figure 20(a) shows a through-thickness schematic of fire damage. Figure 20(b) - 20(e) show representative SEM images of the char layer, an interfacial region between the char layer and unburnt composite, delamination cracks, and a matrix-rich region in the unburnt composite, respectively. The char region was mostly comprised of burnt fibers since the matrix was mostly decomposed. The fibers longitudinally cracked and were detached from the matrix in the combustion front. Delamination was detected in the underlying unburnt layers. The delamination was assumed to be due to the significant difference in thermal conductivities (and coefficients of

thermal expansion) between the charred and underlying composite layers. Finally, the unburnt region of the composite was thermally degraded with few matrix-rich pockets (Mouritz & Mathys, 2001).

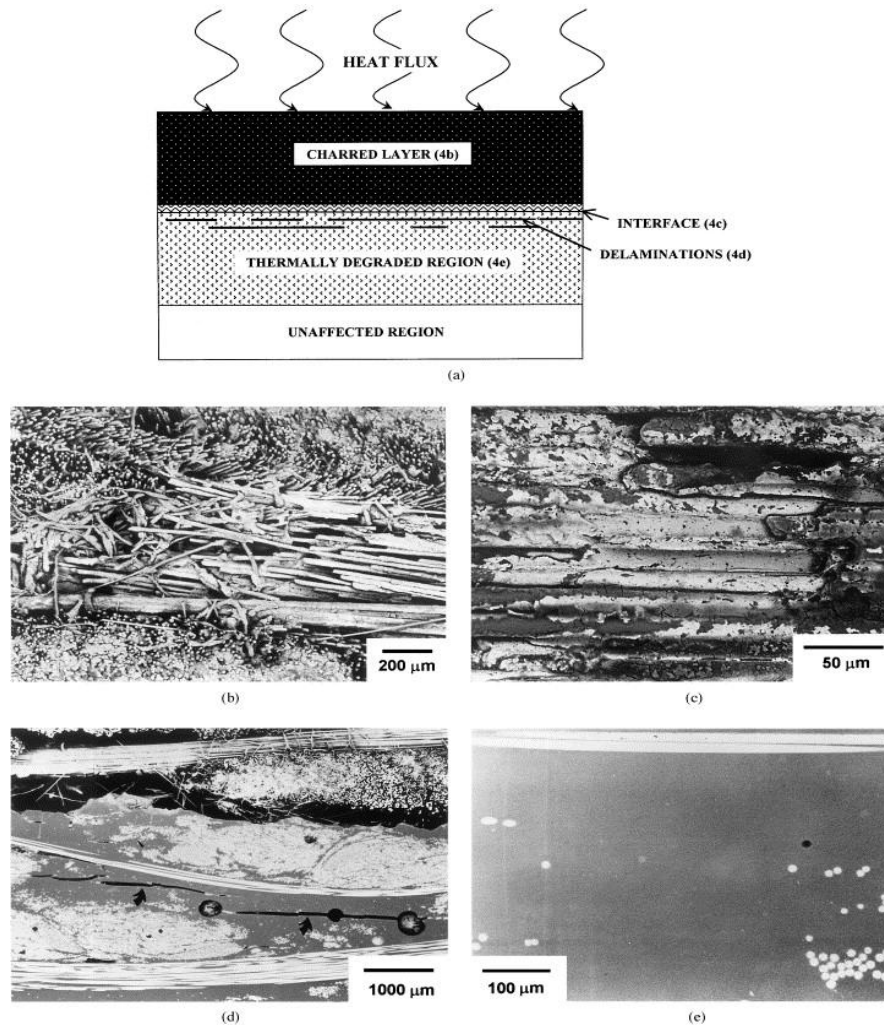


Figure 20. (a) fire damage schematic, (b), (c), (d), and (e) SEM micrographs (Mouritz & Mathys, 2001)

Mouritz (Mouritz, 2003) also investigated the influence of higher heat fluxes and longer fire exposure durations on the post-fire mechanical properties of carbon/epoxy and glass phenolic. These materials were chosen due to their extensive use in modern aircraft. Figure 21 shows a cross-section view of the burnt carbon/epoxy composite laminate. The normalized char thickness in the burnt composite laminate increased substantially with increasing heat flux and heating time, as shown in Figure 22(a) and Figure 22(b) (Mouritz, 2003). As the matrix decomposes to char, the flexural modulus and strength rapidly degraded, as shown in Figure 22(c) and Figure

22(d) (Mouritz, 2003). Overall, carbon/epoxy performed better than glass/phenolic (Mouritz, 2003).

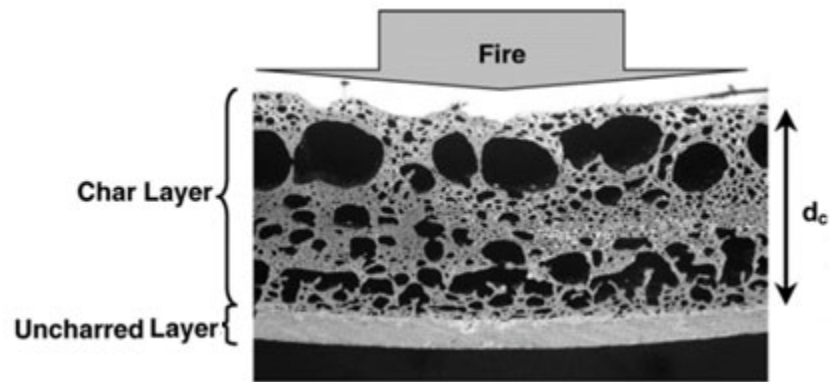


Figure 21. Cross-section view of the carbon/epoxy composite after a fire test (Mouritz, 2003)



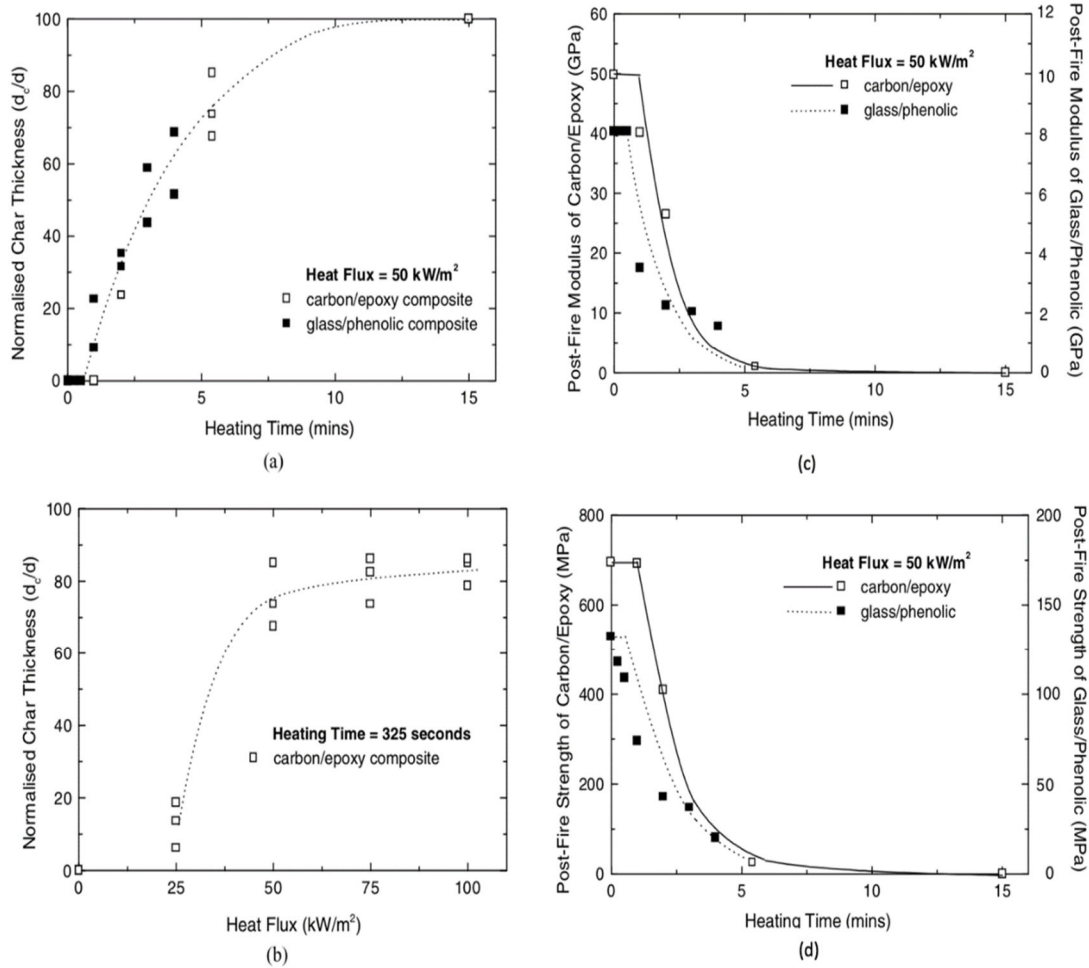


Figure 22. Fire effects on post-fire char thickness, flexural strength, and modulus (Mouritz, 2003)

Mouritz (Mouritz, 2002) investigated the effect of fire on aircraft structural composites' flexural properties using cone calorimetry (Mouritz, 2002; Chen, 2018). Nine different composite systems were considered. Polyester- and phenolic-based matrices were each reinforced with woven Kevlar, woven glass, or chopped glass fibers. Epoxy-based composites were fabricated using woven carbon, woven glass, or chopped glass fibers. The specimens were placed inside a cone calorimeter and exposed to artificial fire at a heat flux of 50 kW/m<sup>2</sup>. Both the polyester- and epoxy-based composites were ignited in a short time (<1 min) after starting the experiment and then burned with a large flame. The phenolic-based composites smoldered for some time before ignition (2.5-7.5 minutes). Fire damage to the polyester and epoxy-based composites was more severe than that for the phenolic-based composites. The polyester and epoxy matrices were entirely decomposed in the charred region.

In contrast, the phenolic matrix appeared to be embrittled and heavily degraded but not wholly consumed due to its low flammability. The flexural properties of the burnt composites were markedly reduced relative to initially undamaged specimens.

Kiel (Kiel, 2006) evaluated the severity of fire exposure on composite on a fuel spill scenario using a cone calorimeter. In this study, two full-scale wings, fabricated from AS4/3501-6 carbon/epoxy composites, were burned for one minute and five-minute exposure times at a heat flux of  $75 \text{ kW/m}^2$ . Four different fire damage zones were identified: the burn through/carbonized zone, the surface alteration zone, the physical distortion zone, and the unaffected composite zone, as shown in Figure 23 (Kiel, 2006). Significant variations in properties were noticed after one minute of fire exposure. The five-minute exposure resulted in a significant loss of the epoxy matrix, fiber damage, and substantial degradation of the composite material (Kiel, 2006). Finally, non-destructive tests showed that the composite materials succumbed to severe thermal damage (Kiel, 2006).

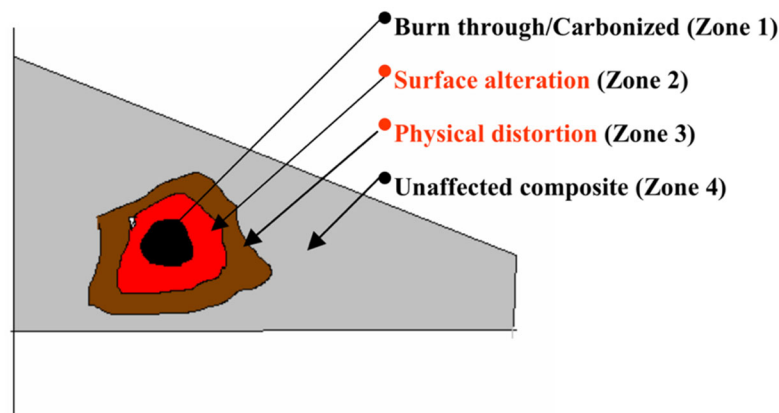


Figure 23. Schematic of typical burn zones due to fire damage (Kiel, 2006)

## 2.2 Surface characterization of composite materials

Aircraft composite materials are often subjected to complex thermomechanical loading during flight, resulting in critical failure of load-bearing components. Since surface characteristics of these materials influence their properties, it is necessary to analyze the modified surfaces to observe changes in composition, shape, chemical, physical, and micromechanical properties (Kar et. al, 1993). Failure analysis is an essential aspect of this process. The determination of the sequence of events that occurred during failure and evaluating the state of stress in the failed part can be achieved through fractography. In these types of analyses, the emphasis is primarily placed on locating the failure-origin and its direction. Crack formation and modes of crack growth due to fatigue are also crucial observations (Floros & Tserpes, 2019; Hojo et al., 1987).

Quantitative measurements of surface topography, plastic deformation, fracture damage, and surface irregularities (e.g., defects) can be performed using imaging techniques *viz.* optical microscopy, confocal microscopy, SEM, and nondestructive inspection techniques *viz.* X-ray computed tomography (CT), pulse-echo C-Scan, and through-transmission ultrasound (TTU) C-Scan (Kar et. al, 1993; Miyoshi, 2002; Walker, 1995).

Optical microscopy at relatively low magnification can be used to identify delaminated surfaces. Specimen preparation for optical microscopy of cross-sections involves sectioning, mounting, and polishing the surface of interest, whereas fracture surface examinations are performed by cutting and cleaning the desired region. It is easier to observe delaminated surfaces in a microscope than translamellar fractures, where the fracture surface is rough and fiber ends are too small for optical microscopy (Kar et. al, 1993). Confocal microscopy is used to characterize surface cracks, pits, wears and craters, oxides, and other debris on the material surface.

SEM is a common technique used for fractography due to its higher magnification, considerable depth of focus, and three-dimensional appearance. The resolution of SEM is usually 100 angstroms (Kar et. al, 1993). Most conventional SEMs can only accommodate small specimen sizes in comparison to an optical microscope. Therefore, large specimens must be partially cut to be characterized by SEM. Moreover, specimen preparation is extensive to minimize the effects of electrical charging, electron beam damage, and outgassing of volatiles. Therefore, optical microscopy is recommended as a less destructive technique before SEM (Kar et. al, 1993).

The techniques discussed above play a significant role in the failure analysis of aircraft structures. A comprehensive fracture analysis process, called the failure analysis logic network, was outlined in the FAA composite failure analysis handbook (Kar et. al, 1993; Walker, 1995). The steps involved are outlined in Figure 24. As an exercise to determine the failure analysis logic network (see Figure 24), the steps outlined in it were performed by Boeing on an angle component provided by the USAF. Using fractography and other non-destructive tests, Boeing successfully identified the material system (resin composition-from spectroscopic analyses), stacking sequence, and failure characteristics of the component (Walker, 1995).

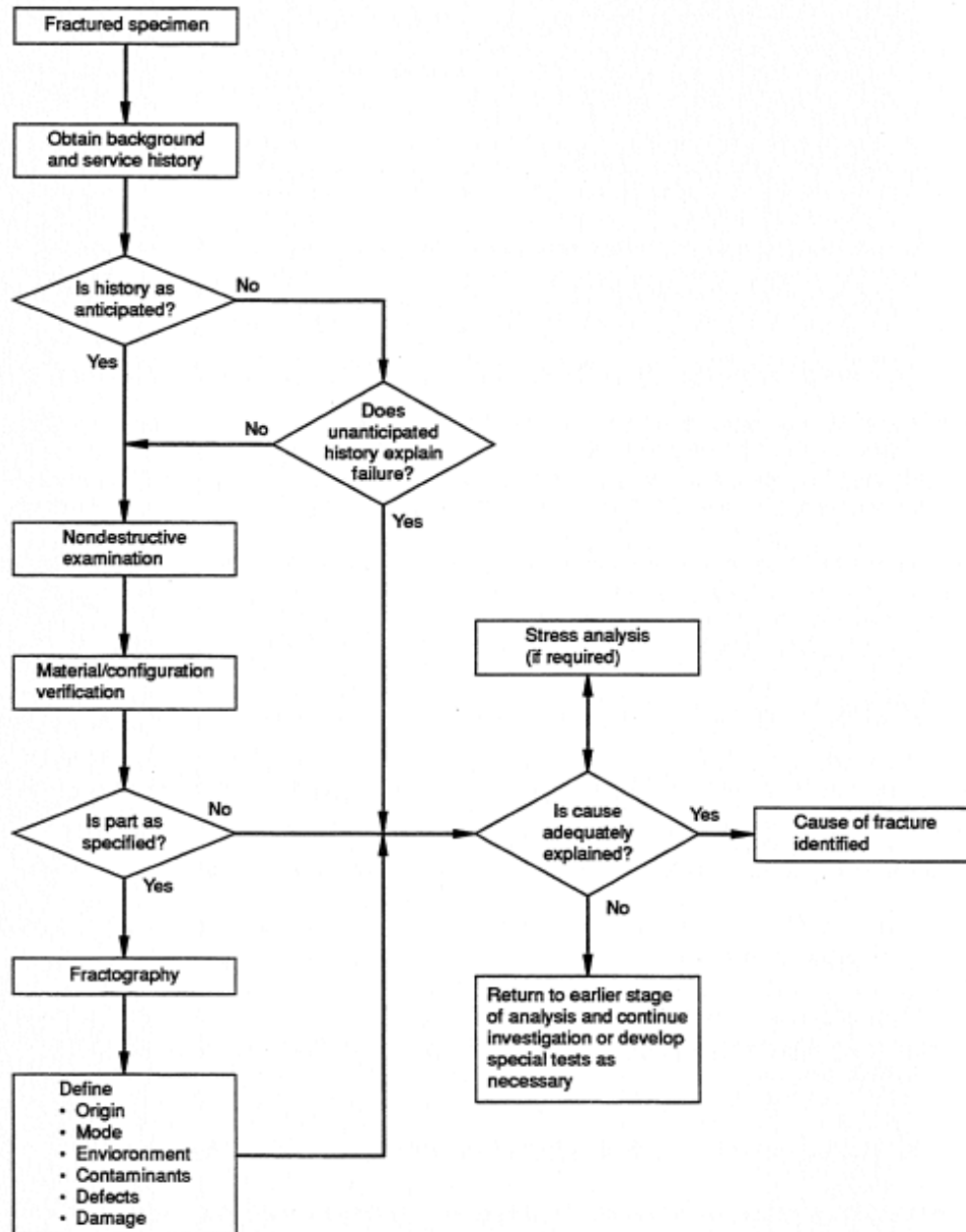


Figure 24. Fracture analysis logic network (Walker, 1995)

## 2.3 Surface characterization of thermally degraded composites

Surface characteristics of aircraft composites with thermal damage can be evaluated using both fractography and NDI techniques. Additionally, chemical defects like contaminants (carbon by-products/char) can be analyzed using infrared spectroscopy. Wolfrum (Wolfrum et al., 2009) studied the effect of long-term thermal degradation of carbon-fiber epoxy composites on their strength characteristics. Quasi-isotropic IM7/8552 and G939/M18-1 specimens were subjected to

isothermal aging in standard convection ovens at 180, 190, 200 °C for 500 days. The specimens were subjected to tensile, compressive, and interlaminar shear (ILS) tests. The degradation of matrix constituents was evaluated using IR spectroscopy, followed by SEM investigations of the fracture surface and cross-sections of the specimens (Wolfrum et al., 2009).

The SEM micrographs shown in Figure 25 represent the surface characteristics of the aged (8552-200 °C, 69 days, M18-1/939-200 °C, 34 days) and unaged ILS specimens of two materials. The surface of the aged specimens exhibited micro-cracking, which resulted in local delaminations. The matrix-to-fiber adhesion of the unaged specimens was better than the aged specimens, as shown in Figure 25(a) and Figure 25(c), resulting in the separation of the fibers from the matrix as shown in Figure 25(d) (Wolfrum et al., 2009).

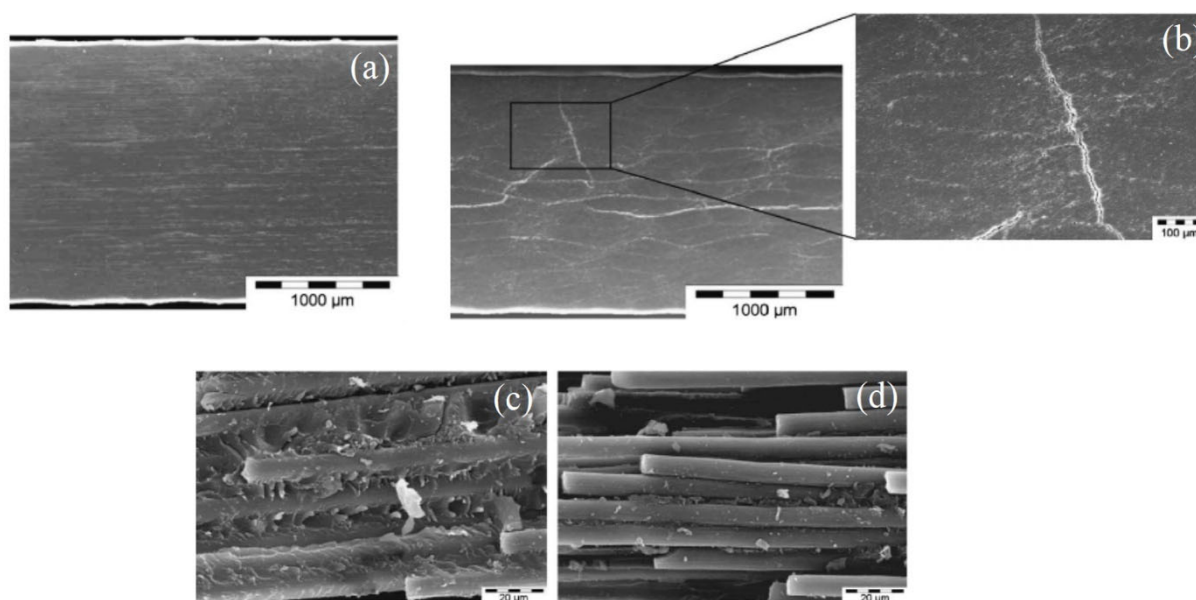


Figure 25. SEM of cross-sections showing the effects of aging (Wolfrum et al., 2009)

Grange (Grange et al., 2018) studied the thermophysical properties of carbon-fiber-reinforced polymers and thermal degradation at higher temperatures (up to 1000 °C). The carbon/PEKK samples exhibited recrystallization of the resin and a certain level of surface delamination resulting in the persistence of the fiber-matrix surface. Also, the carbon/epoxy specimens had the least residual amount of matrix, resulting in the fibers' complete exposure. The carbon/phenolic samples possessed a decomposed matrix on the burnt surface, protecting the surface from further thermal degradation (Grange et al., 2018). The thermally degraded specimen surfaces for the three material systems are shown in Figure 26. In the case of carbon/PEKK in Figure 26(a), it was reported that the surface possesses visible delamination while upholding the adhesion

between the matrix and fibers. This phenomenon was attributed to matrix recrystallization, further indicating that the residual non-decomposed matrix is a reason for better mechanical and thermal properties (Grange et al., 2018). However, for the carbon/phenolic specimens in Figure 26(b), there is a certain level of matrix decomposition that contributes to its thermal properties. The carbon/epoxy specimens in Figure 26(c) exhibited the most matrix degradation resulting in poor mechanical and thermal properties, with an almost total exposure of the fibers (Grange et al., 2018).

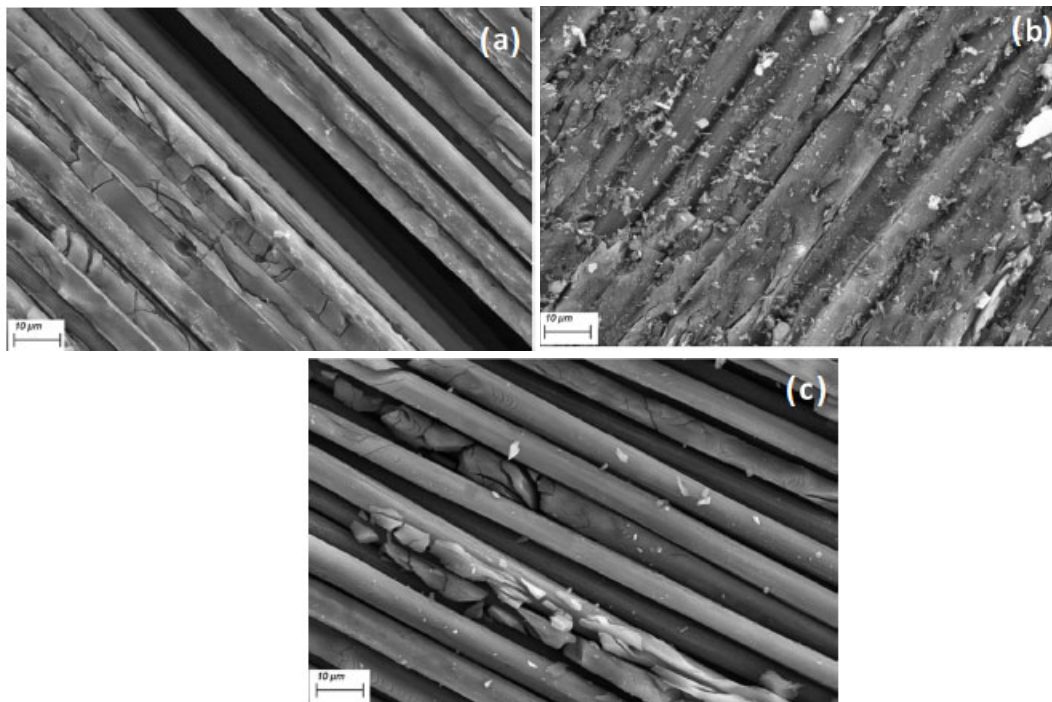


Figure 26. Micrographs showing surfaces of degraded samples at 1000 °C (Grange et al., 2018)

Tadini (Tadini et al., 2017) also conducted TGA experiments on PEKK-based carbon composites and phenolic-carbon composites subjected to fracture before thermal degradation. The virgin PEKK crash samples reportedly exhibited a few exposed fibers due to failure, whereas in the post TGA samples, matrix recrystallization leads to the bundling of the exposed fibers. This phenomenon was absent in the carbon/phenolic samples. Moreover, the difference between the virgin and the TGA samples for the carbon/phenolic samples was less apparent, as shown in the SEM micrographs in Figure 27 (Tadini et al., 2017).



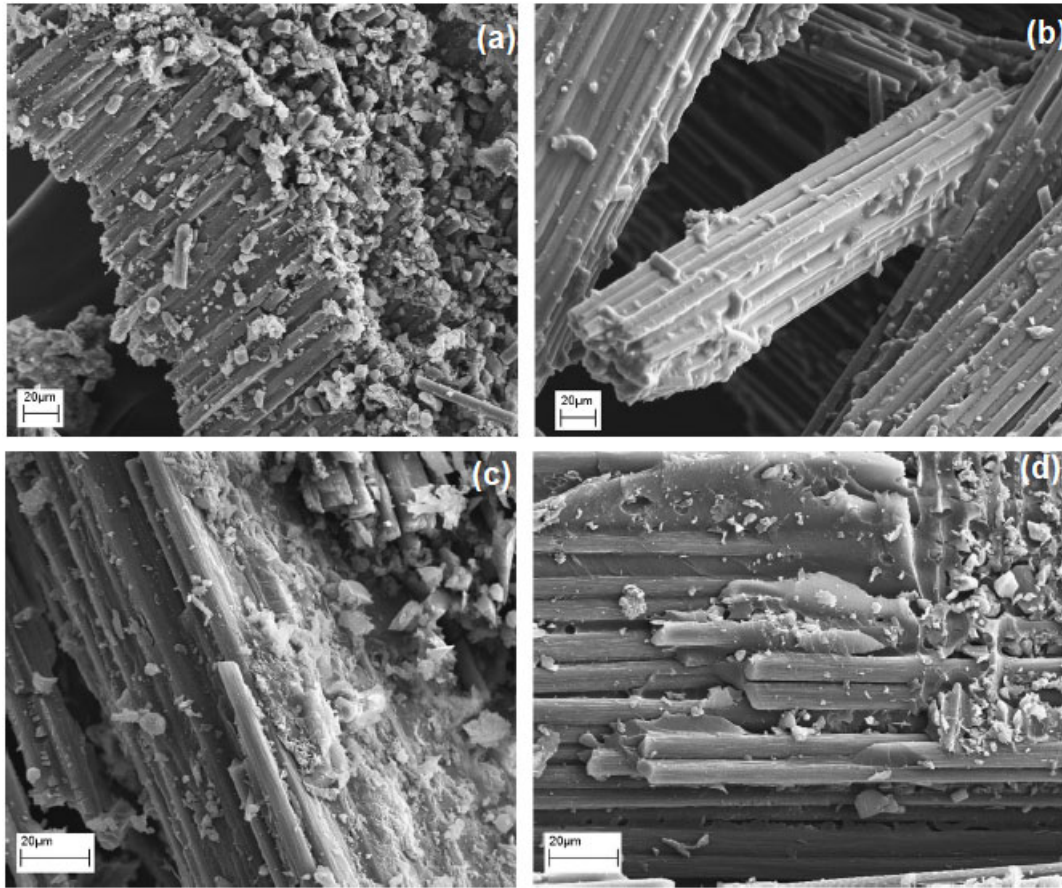


Figure 27. Micrographs of the crash specimens (a), (c) Before, (b),(d) After TGA (Tadini et al., 2017)

Liu (Liu et al., 2016) investigated the localized damage response of CFRP composite sandwich panels after thermal exposure. The panels were fabricated by the hot-press molding method, followed by exposure to various temperatures (20, 250, 280 °C) for a fixed time of six hours. The inner core of the sandwich panels consisted of pyramidal trusses fabricated by the hot-press molding method. The absorbed energy, failure mechanism, and the magnitude of indentation load had decreased with the increase in exposed temperature, due to the higher level of matrix degradation and poor matrix fiber-interface properties; this trend is shown in the SEM micrographs of the test specimens in Figure 28 (Liu et al., 2016).

Additionally, Liu (Liu et al., 2014) also worked on CFRP pyramid-truss-core sandwich panels exposed to 300 °C for six hours. The high temperature and exposure time resulted in reductions in compression modulus and strength. Additionally, thermal exposure also caused delamination and low matrix-to-fiber adhesion. The modulus and strength were predicted at different temperatures and exposure times, with experimental results in good agreement with the predicted values (Liu et al., 2014).

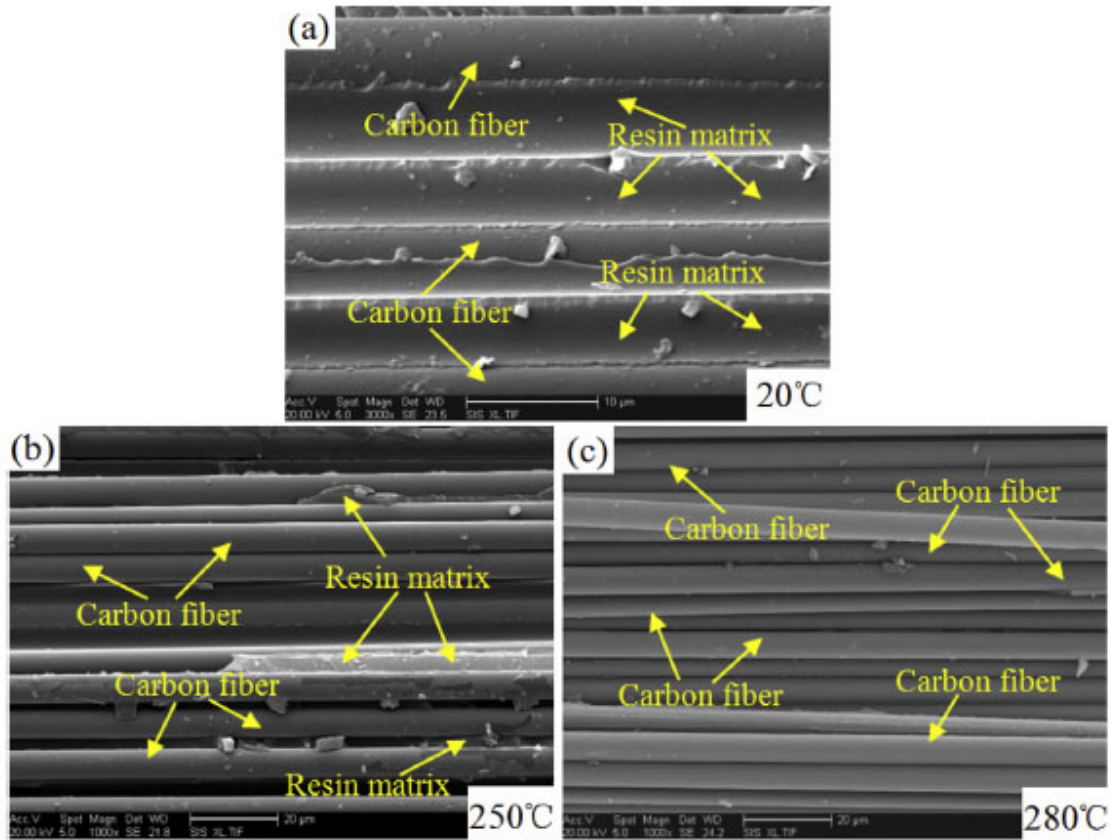


Figure 28. Micrographs of fiber-matrix interfaces showing thermal exposure (Liu et al., 2016)

Composite materials exposed to flame can be damaged catastrophically. The extent of fire-damage is dependent on flame properties. The behavior of aircraft composites exposed to the flame was examined by Schuhler (Schuhler et al., 2018). In this study, thermoset and thermoplastic laminates were exposed to a flame with a constant high-heat flux of  $106 \text{ kW/m}^2$ , representing an extreme-fire condition.

Post-fire microscopy was performed on the samples to analyze the surface morphology. In carbon/epoxy samples, significant char formation caused a tremendous mass loss, resulting in dry and exposed fibers. PPS-based samples burned rapidly to develop voids. The voids acted as barriers to energy absorption, leading to lower temperatures at the unexposed surface. Figure 29(a) and Figure 29(b) show the numerical analysis results, and Figure 29(c) and Figure 29(d) show the fire reaction mechanisms for these two systems (Schuhler et al., 2018).



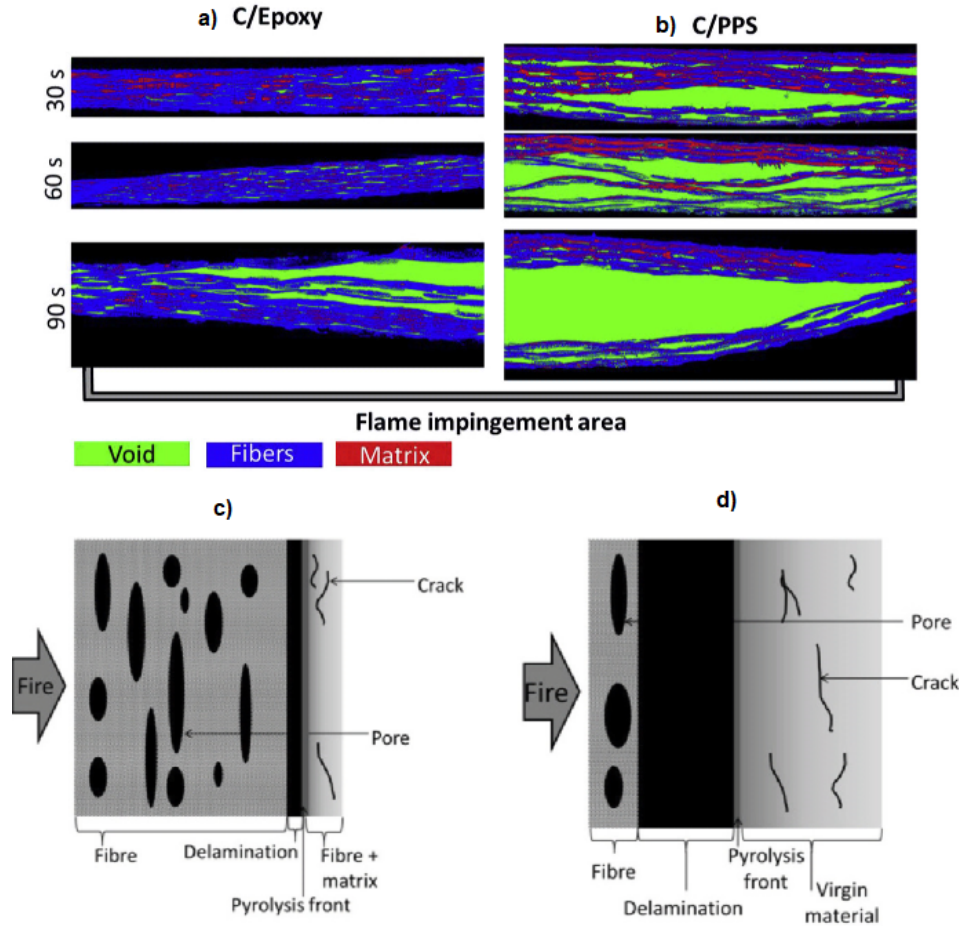


Figure 29. (a),(b) Through thickness micrographs, (c),(d) Reaction mechanism schematics (Schuhler et al., 2018)

Further work on PPS laminates was performed by Maaroufi (Maaroufi et al., 2017). Carbon/PPS woven-ply laminates were exposed to fires of varying heat fluxes from 20-50 kW/m<sup>2</sup>. Ultrasonic C-Scans quantified local delamination. Compressive damage resulted in fire-induced delamination and the onset of local kink-bands during compressive loadings and, ultimately, plastic buckling (Maaroufi et al., 2017). The C-scan maps of the specimens provided information on the damage mechanisms post-compression. These images are shown in Figure 30 (Maaroufi et al., 2017). Similar work on carbon/epoxy and carbon/PPS aircraft composites were undertaken by Benoit (Benoit et al., 2015). The melted PPS matrix protects the carbon fibers from further oxidation and further strength degradation. Furthermore, oxidation and a decrease in fibrous reinforcement may dramatically decrease in strength and modulus (Benoit et al., 2015).

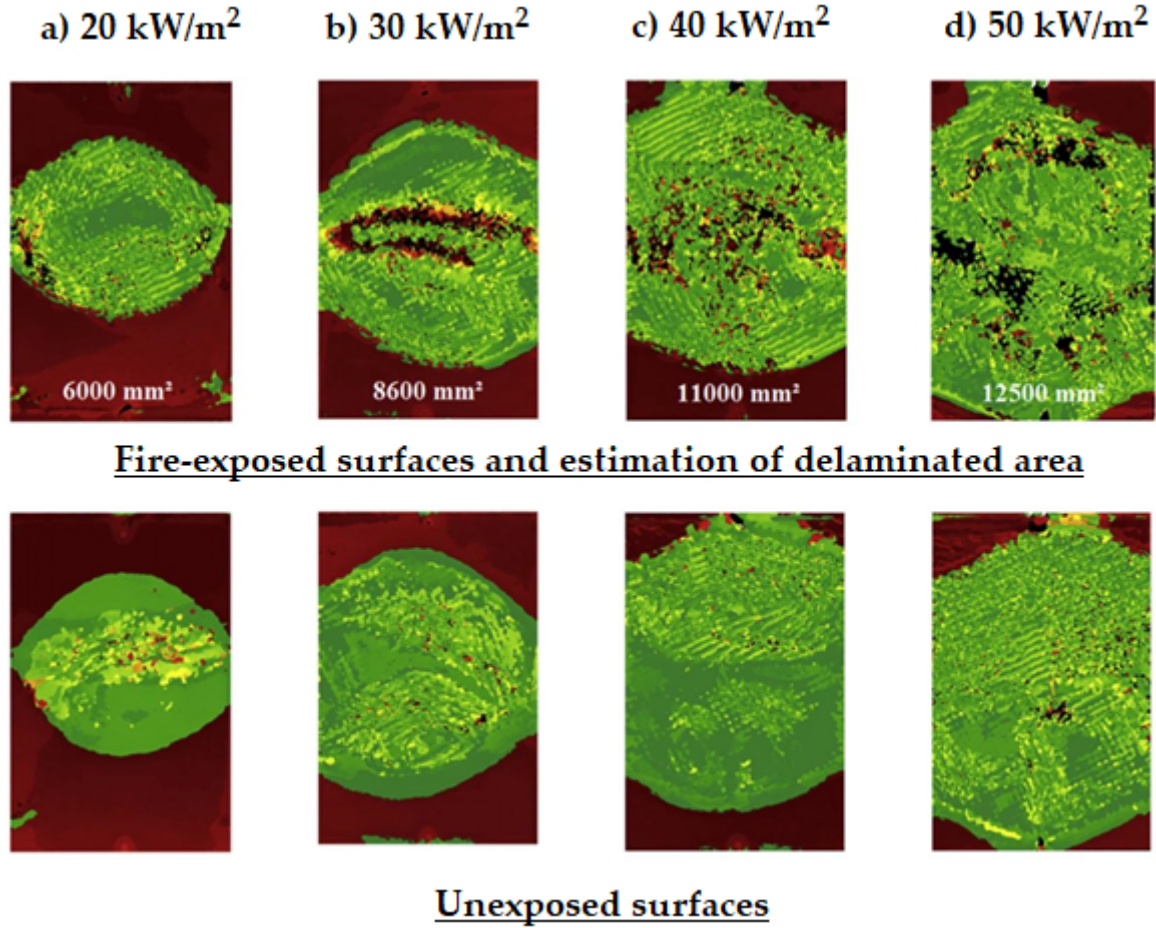


Figure 30. Ultrasonic C-Scans of carbon/PPS laminates in compressive loadings after fire (Maaroufi et al., 2017)

## 2.4 Char removal techniques

Pyrolysis is widely used for recycling and recovering fibers from scrap composites (Fernández et al., 2018; Yang et al., 2012). It involves the thermo-chemical decomposition of the composite's organic matrix at temperatures in the range of 450 - 700 °C in an inert environment. The temperature levels are dependent on the matrix since 450 °C is used on the pyrolysis process of polyester-based, and up to 550 °C is used for epoxy-based composite materials (Yang et al., 2012). Elevated temperatures profoundly degrade the mechanical properties of the fibers (Fernández et al., 2018; Yang et al., 2012). Due to the high temperatures used in pyrolysis, char is deposited on the surface of recycled fibers. Pyrolysis is usually combined with an oxidation process to remove the deposited chars and obtain clean fibers. The combined pyrolysis and oxidation process occurs in thermolysis equipment, which consists of a heating system (for pyrolysis) and a gas condensation device (for oxidation). The oxidation time should be carefully optimized to avoid degradation of fiber mechanical properties.

Fernandez (Fernández et al., 2018) optimized the pyrolysis and oxidation processes on scrap HexPly F593 supplied by Airbus. The HexPly F593 is a plain-woven prepreg made of epoxy resin reinforced with Toray T300/ 3k carbon fibers, and is widely used in the aeronautical industry. Severe damage to the fibers was observed once the temperature exceeded 500°C during pyrolysis. The oxidation was optimized by varying the time from 30 to 90 minutes. The main goal of this optimization was to remove the chars deposited on the fiber surface without affecting their microstructure and mechanical properties. The presence of char on the fiber surfaces was assessed using SEM images. SEM images of both pristine fibers and recycled fibers at oxidation times of 30, 60, and 90 minutes are shown in Figure 31 (Fernández et al., 2018). The pristine fibers' morphology is rough and has irregularities while it is smooth and regular and has no minor evidence of chars in the recycled fibers. Also, no damage was detected. Therefore, short oxidation times (i.e., 30 minutes) were efficient for char removal.

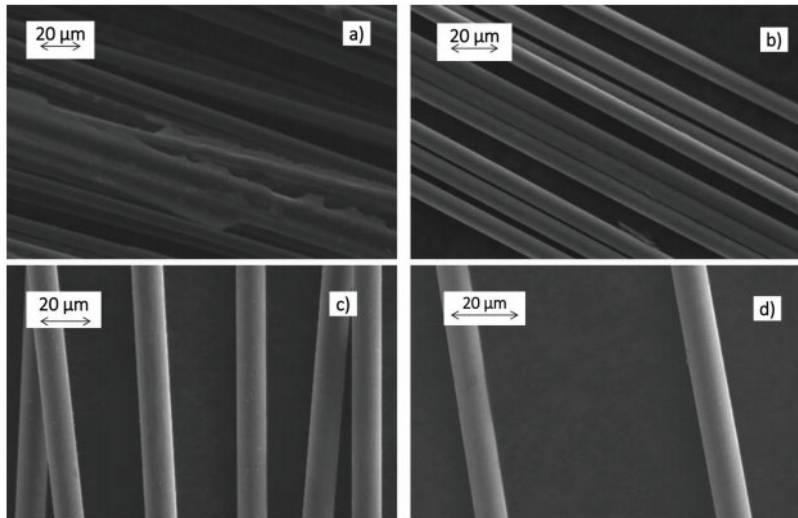


Figure 31. SEM images of the carbon fibers before and after recovery (Fernández et al., 2018)

Chemical products available over-the-counter can also be used for removing chars and other fire by-products (i.e., carbon build-up) that develop on the surface of burnt fibers. While very little to no information is available on chemical products used for dissolving char and other fire byproducts on composite materials, several solvents (see Table 1) for removing char from metallic surfaces (i.e., stainless steel, nickel steel, copper, aluminum, brass, cast iron) are commercially available. The chemical composition of these commercially available products can form the basis for developing similar solvents to remove char and other fire by-products from composites fiber ends.

Table 1. List of chemical solvents and commercially available products for char removal

Product Name	Applications	Chemical composition
Carbon-off! (Carbon-off!, 2019)	Excellent for removing char from metallic surfaces (brass, stainless steel, nickel steel, <i>etc.</i> ), used in high-temperature cookware.	Dichloromethane (75-09-2), Ethanol (67-17-5), Methyl Alcohol (67-56-1), Aromatic Hydrocarbon (108-88-3), 2-Butoxyethanol (111-76-2), Ammonia (7664-41-7), Propane/n-Butane (68476-86-8).
Chem-Dip carburetor and parts cleaner (Chem-Dip, 2019)	Highly effective at removing char and fuel combustion by-products (gum, varnish, fuel residue) from carburetor parts in 15-30 minutes without heat, aeration, or agitation. Safe for use with most plastic and metallic parts, including steel, aluminum, and their alloys.	Heterocyclic and Aliphatic Amines (Mixture), 2-Butoxyethanol (11-76-2), 2-(2-Butoxyethoxy) ethanol (112-34-5), and Ethoxylated Alkyl Amines (Mixture)
Carbona 2-In 1 oven rack & grill cleaner (Carbona, 2019)	Effective at removing chars from oven rack and grills.	< 5% anionic surfactants.
Zep heavy-duty oven & grill cleaner (ZEP, 2019)	The thick foam dissolves char, combustion by-products, and grease on contact from oven and grill surfaces. Suitable for use on stainless steel, porcelain, and ceramics.	Water (Solvent), Ethanolamine (Solvent), Butane (Propellant), Triethanolamine (Detergent Additive), Tri-Propylene Glycol Methyl Ether (Solvent), Propylene Glycol (Solvent), Magnesium Aluminum Silicate (Absorbent), Propane (Propellant); Potassium Hydroxide (Ph Adjuster), Butoxyethanol (Solvent)

Another technique to remove char from burnt composites is cold jet ice blasting. The dry ice blasting technique was used mainly to clean char from wood, bricks, metals, and ceramics (ColdJet). Dry ice blasting, similar to sandblasting, uses a pressurized air stream to clean a surface without damaging the underlying material, as shown in Figure 32 (ColdJet). Cold jet dry ice blasting uses soft dry ice (carbon dioxide, CO<sub>2</sub>) accelerated at a supersonic speed. This process can potentially use a compressed air supply of 80 psi/50 scfm. When the solid dry ice reaches the surface, it creates a small explosion lifting the undesirable layer (char) without damaging active electrical or mechanical parts or creating fire hazards. Dry ice blasting is a non-abrasive, non-flammable, and non-conductive cleaning method. The dry ice transforms from a

solid to gas upon reaching the surface, and it produces local high shear stresses between the micro-layers. This phenomenon happens over a short duration, causing a rapid micro-crack propagation between the layers. The gas expands to about 800 times the volume of the solid CO<sub>2</sub> pellet in a millisecond, causing a “micro-explosion.” The micro-explosion lifts the thermally fractured coating particles (char) from the substrate (ColdJet). The gas expands outward along the surface and results in an "explosion shock front," creating a high pressure between the surface and the thermally fractured coating particles carrying the particles away from the surface (ColdJet).

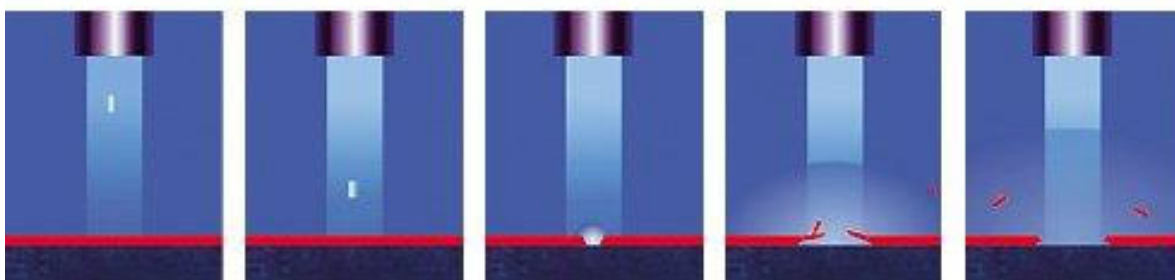


Figure 32. Cold jet ice blasting steps (ColdJet)

Ultrasonication might also be useful for char removal. Ultrasonication uses ultrasound energy to agitate the particles in a sample using ultrasonic frequencies. This agitation leads to sonochemistry that arises from acoustic cavitation, as shown in Figure 33. Sonochemistry can be introduced through three phases: formation of the bubbles, growth of the cavitation bubbles, and the collapse of bubbles resulting in an implosion of bubbles (EpiSonic). Placing a specimen inside the sonicator filled with a liquid solution and initiating ultrasonic irradiation produce a cavitation bubble that grows in time. Once the bubble collapses, a shearing force is produced, resulting in char removal from the burnt composite materials. The collapsing bubbles also generate very high temperatures for shorter periods. Thus, significant energy is absorbed by the surface while the overall sample does not appreciably warm to higher temperatures. The ultrasonication process is illustrated in Figure 34 (EpiSonic).



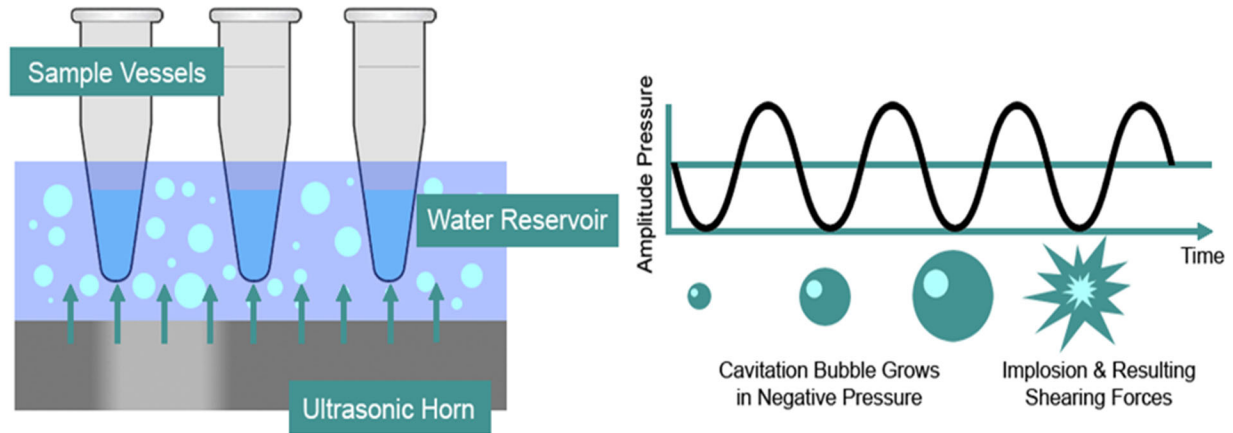


Figure 33. Schematic showing the ultrasonication process (EpiSonic)



Figure 34. Flow diagram showing the physics of ultrasonication

### 3 Conclusion

This literature review provides details about the effects of fire and elevated temperatures on fiber-reinforced composites. This report summarizes the following

- i) Experimental testing on composite materials with applications to commercial aircraft and ships.
- ii) Fire damage mechanisms that occur when exposing a composite material to controlled open flame or heat fluxes.
- iii) NDI and destructive inspection techniques for assessing the severity and extent of thermal degradation.
- iv) Chemical and physical techniques that can be used to remove char and other fire by-products from burnt composites.

Fire effects on composite materials include matrix and organic fibers decomposition/pyrolysis, porosity formation due to volatile outgassing from matrix decomposition, delamination, matrix cracking, and char formation. Fire can also drastically degrade the mechanical properties of composite materials and alter the features and morphology of their failed surfaces in ways that obscure relevant structural fracture characteristics.

Small- and large-scale fire-exposure and char removal experiments are currently being performed to remove char from the burned fiber ends and expose the underlying fracture surface characteristics. The goal is to eventually create a comprehensive fire-forensic analysis protocol that can be used to identify the root cause of failure in aircraft in the event of a crash. The existing FAA composite failure analysis handbook (Kar et. al, 1993) will be updated with instructions on the sequence of steps involved in evaluating the cause of failure in composites exposed to post-crash fire.

## 4 References

- Alderliesten, R. (2015). Designing for damage tolerance in aerospace: A hybrid material technology. *Materials & Design*, 66, 421-428.
- Anjang, A., Chevali, V., Kandare, E., Mouritz, A., & Feih, S. (2014). Tension modelling and testing of sandwich composites in fire. *Composite Structures*, 113, 437-445.
- Benoit, V., Alexis, C., Clément, K., Garda, M., Quentin, V., & Eric, D. (2015). Correlation between post fire behavior and microstructure degradation of aeronautical polymer composites. *Materials & Design*, 74, 76-85.
- Botelho, E. C., Silva, R. A., Pardini, L. C., & Rezende, M. C. (2006). A review on the development and properties of continuous fiber/epoxy/aluminum hybrid composites for aircraft structures. *Materials Research*, 9(3), 247-256.
- Brown, A. (2013). *The Decomposition Behavior of Thermoset Carbon Fiber Epoxy Composites in the Fire Environment*.
- Brown, A., Jernigan, D. A., & Dodd, A. B. (2015). *Intermediate-Scale Fire Performance of Composite Panels under Varying Loads*. <https://www.osti.gov/biblio/1177721>
- Brown, A., Dodd, A., & Erickson, L. (2012). *The Behavior of Carbon Fiber-Epoxy Based Aircraft Composite Materials in Unmitigated Fires*. Paper presented at the 34 th Symposium on Combustion, Warsaw, Poland.
- Brown, A. L., Dodd, A. B., & Pickett, B. M. (2011). *Intermediate Scale Composite Material Fire Testing*. Paper presented at the ASME 2011 International Mechanical Engineering Congress and Exposition.
- Caccese, V., Mewer, R., & Vel, S. S. (2004). Detection of bolt load loss in hybrid composite/metal bolted connections. *Engineering Structures*, 26(7), 895-906.

- Camino, G., Costa, L., & Martinasso, G. (1989). Intumescent fire-retardant systems. *Polymer Degradation and Stability*, 23(4), 359-376.
- Chen, Z.-M. (Producer). (2018, june 26, 2018). Composite failure analysis after post-crash fire. [Powerpoint Presentation, presented to Mississippi State University, Miss. State, USA]
- EpiSonic. EpiSonic Multi-Functional Bioprocessor 1100. Retrieved from <https://www.epigentek.com/catalog/episonic-multi-functional-bioprocessor-1100-p-2997.html>
- FAA. (2018). *Airframe, Aviation Maintenance Technician Handbook , Vol. 2 (FAA-H-8083-31)*.
- Fernández, A., Lopes, C. S., González, C., & López, F. A. (2018). Characterization of carbon fibers recovered by pyrolysis of cured prepregs and their reuse in new composites. In *Recent Developments in the Field of Carbon Fibers: IntechOpen*.
- Florio Jr, J., Henderson, J. B., Test, F. L., & Hariharan, R. (1991). A study of the effects of the assumption of local-thermal equilibrium on the overall thermally-induced response of a decomposing, glass-filled polymer composite. *International Journal of Heat and Mass Transfer*, 34(1), 135-147.
- Floros, I., & Tserpes, K. (2019). Fatigue crack growth characterization in adhesive CFRP joints. *Composite Structures*, 207, 531-536.
- Gillian, L., Valentin, B., Julien, B., and Cedric, Huchette (Producer). (2017). Fire properties and behavior of composite materials. *ONERA*. [Powerpoint Document]
- Grange, N., Tadini, P., Chetehouna, K., Gascoin, N., Reynaud, I., & Senave, S. (2018). Determination of thermophysical properties for carbon-reinforced polymer-based composites up to 1000° C. *Thermochimica Acta*, 659, 157-165.
- Greenhalgh, E. (2009). *Failure analysis and fractography of polymer composites*: Elsevier.
- Guimarães, T. A., Silva, H. L., Rade, D. A., & Cesnik, C. E. (2020). Aeroelastic Stability of Conventional and Tow-Steered Composite Plates Under Stochastic Fiber Volume. *AIAA Journal*, 58(6), 2748-2759.
- Hode, J. C. (2012). *Development of a Firefighting Agent Application Test Protocol for Aircraft Fuselage Composites, Phase I-Carbon Fiber*.



- Hojo, M., Tanaka, K., Gustafson, C. G., & Hayashi, R. (1987). Effect of stress ratio on near-threshold propagation of delamination fatigue cracks in unidirectional CFRP. *Composites Science and Technology*, 29(4), 273-292.
- Horner, A. (2000). *Aircraft materials fire test handbook*. (Publication No. DOT/FAA/AR-00/12). <https://www.fire.tc.faa.gov/handbook>
- Hubbard, J. A., Brown, A., & Dodd, A. B. (2011). *Carbon fiber composite characterization in adverse thermal environments*.
- Johnston, A., Jodoin, A., & MacLaurin, J. (2000). *Evaluation of fire performance of composite materials for aircraft structural applications*: Society of Manufacturing Engineers.
- Kabche, J. P. (2006). *Structural Testing and Analysis of Hybrid Composite/Metal Joints for High-Speed Marine Structures*. The University of Maine,
- Kar, R. J., Wright Laboratory (Wright-Patterson Air Force Base, Ohio), Federal Aviation Administration Technical Center (U.S.), & Purdue University. (1993). Composite failure analysis handbook. Wright-Patterson Air Force Base, OH: Materials Directorate, Wright Laboratory, Air Force Systems Command.
- Kar, R. (1992). *Composite Failure Analysis Handbook. Volume 2: Technical Handbook. Part 1- Procedures and Techniques*. <https://apps.dtic.mil/sti/citations/ADA250521>
- Kiel, J. A. F. R. L., Fire Research Group, ARFF Working Group (Producer). (2006). AFRL Fire Research Group Capabilities and Research on Aerospace Composite Materials.
- Kumar, L. M., Usha, K., & Chakravarthy, P. (2018). *Advanced Ablative composites for Aerospace applications*. Paper presented at the IOP Conference Series: Materials Science and Engineering.
- Liu, J., Kan, T., Lou, J., Xiang, L., Zhu, X., & Tang, Y. (2016). Localized damage response of carbon fiber reinforced polymer composite sandwich panel after thermal exposure. *Polymer Testing*, 50, 33-40.
- Liu, J., Zhu, X., Zhou, Z., Wu, L., & Ma, L. (2014). Effects of thermal exposure on mechanical behavior of carbon fiber composite pyramidal truss core sandwich panel. *Composites Part B: Engineering*, 60, 82-90.
- Maaroufi, M., Carpier, Y., Vieille, B., Gilles, L., Coppalle, A., & Barbe, F. (2017). Post-fire compressive behaviour of carbon fibers woven-ply Polyphenylene Sulfide laminates for aeronautical applications. *Composites Part B: Engineering*, 119, 101-113.

- Majlingová, A., & Jinb, D. K. Q. X. C. (2018). Current trends in flame-retardant treatment of selected polymers—a review. *Earth*, 2, 0.
- Mouritz, A. (2003). Fire resistance of aircraft composite laminates. *Journal of materials science letters*, 22(21), 1507-1509.
- Mouritz, A. (2006). Fire safety of advanced composites for aircraft. *ATSB Research and Analysis Report, Australian Transport Safety Bureau, Aviation Safety Research Grant no. B2004/0046*.
- Mouritz, A. (2002). Post-fire flexural properties of fibre-reinforced polyester, epoxy and phenolic composites. *Journal of Materials Science*, 37(7), 1377-1386.
- Mouritz, A., & Gardiner, C. (2002). Compression properties of fire-damaged polymer sandwich composites. *Composites Part A: Applied Science and Manufacturing*, 33(5), 609-620.
- Mouritz, A., Gardiner, C., Mathys, Z., & Townsend, C. (2001). Post-fire properties of composites burnt by cone calorimetry and large-scale fire testing. *Proceeding of the ICCM13, Beijing, China*.
- Mouritz, A., & Gibson, A. (2007). *Fire properties of polymer composite materials* (Vol. 143): Springer Science & Business Media.
- Mouritz, A., & Mathys, Z. (2001). Post-fire mechanical properties of glass-reinforced polyester composites. *Composites Science and Technology*, 61(4), 475-490.
- Miyoshi, K. (2002). Surface Characterization Techniques: An Overview. (Publication No. NASA/TM-2002-211497).  
<https://ntrs.nasa.gov/api/citations/20020070606/downloads/20020070606.pdf?attachment=true>
- Ochs, R. (2010). Development of the next generation fire test burner for powerplant fire testing applications. *Proceeding of IASFPWG, London, UK*.
- Ochs, R., Hode, J. C. (n.d.). Federal Aviation Composite Material Fire Fighting. Retrieved December 3, 2021, from <https://www.fire.tc.faa.gov/pdf/materials/June09Meeting/hode-0609-CompositeFuselageFirefightingWork.pdf>.
- Phil, E., & Soutis, C. (2014). *Polymer composites in the aerospace industry*: Elsevier.

- Popescu, C. M., & Pfriem, A. (2020). Treatments and modification to improve the reaction to fire of wood and wood based products—An overview. *Fire and Materials*, 44(1), 100-111.
- Puchades, M. I. G. (2016). *Behaviour of composite sandwich decks at high temperatures*.
- Ray, S. S., & Kuruma, M. (2019). *Halogen-free flame-retardant polymers: next-generation fillers for polymer nanocomposite applications* (Vol. 294): Springer Nature.
- Rouchon, J. a. B., MJ. (May 2009). Fatigue and damage tolerance evaluation of structures: the composite materials response. Rotterdam, The Netherlands.
- Sarkos, C. (2011). *Improvements in aircraft fire safety derived from FAA research over the last decade*. (Publication No. DOT/FAA/AR-TN11/8). <https://www.fire.tc.faa.gov/pdf/TN11-8.pdf>
- Schuhler, E., Coppalle, A., Vieille, B., Yon, J., & Carpier, Y. (2018). Behaviour of aeronautical polymer composite to flame: A comparative study of thermoset-and thermoplastic-based laminate. *Polymer Degradation and Stability*, 152, 105-115.
- Sun, H.-T., Chang, F.-K., & Qing, X. (2002). The response of composite joints with bolt-clamping loads, Part I: Model development. *Journal of Composite Materials*, 36(1), 47-67.
- Tadini, P., Grange, N., Chetehouna, K., Gascoin, N., Senave, S., & Reynaud, I. (2017). Thermal degradation analysis of innovative PEKK-based carbon composites for high-temperature aeronautical components. *Aerospace Science and technology*, 65, 106-116.
- Torre, L., Kenny, J., Boghetich, G., & Maffezzoli, A. (2000). Degradation behaviour of a composite material for thermal protection systems Part III Char characterization. *Journal of Materials Science*, 35(18), 4563-4566.
- Tranchard, P., Samyn, F., Duquesne, S., Thomas, M., Estèbe, B., Montès, J.-L., & Bourbigot, S. (2015). Fire behaviour of carbon fibre epoxy composite for aircraft: Novel test bench and experimental study. *Journal of Fire Sciences*, 33(3), 247-266.
- Walker, G. (1995). Composite Failure Analysis Handbook Update (Final Report, Aug. 1990-Apr. 1995).
- Wolfrum, J., Eibl, S., & Lietch, L. (2009). Rapid evaluation of long-term thermal degradation of carbon fibre epoxy composites. *Composites Science and Technology*, 69(3-4), 523-530.

- Wright, M. T., Luers, A. C., Darwin, R. L., Scheffey, J. L., & Bowman, H. L. (2003). *Composite Materials in Aircraft Mishaps involving Fire: a Literature Review*.
- Yang, Y., Boom, R., Irion, B., van Heerden, D.-J., Kuiper, P., & de Wit, H. (2012). Recycling of composite materials. *Chemical Engineering and Processing: Process Intensification*, 51, 53-68.
- Zhuguo, Z., Yingchun, Z., & Xupo, O. (2011). Study on key certification issues of composite airframe structures for commercial transport airplane. *Procedia Engineering*, 17, 247-257.